Experimental Gas Phase ^{1}H NMR Spectra and Basis Set Dependence of *ab initio* GIAO MO Calculations of ^{1}H and ^{13}C NMR Absolute Shieldings and Chemical Shifts of Small Hydrocarbons

Thomas Zuschneid, Holger Fischer, Thomas Handel, Klaus Albert, and Günter Häfelinger

Institut für Organische Chemie, Universität Tübingen, Auf der Morgenstelle 18, D-72076 Tübingen

Reprint requests to Prof. Dr. G. Häfelinger. E-Mail: guenter.haefelinger@uni-tuebingen.de

Z. Naturforsch. **59b,** 1153 – 1176 (2004); received February 6, 2003

High-resolution gas phase measurements of ^{1}H NMR spectra at 400 MHz and atmospheric pressure of seven small hydrocarbons are presented. The developed new method and the experimental set-up are described. *Ab initio* GIAO MO calculations of ^{1}H and ^{13}C NMR absolute shieldings on the HF, MP2 and B3LYP levels using 25 standard gaussian basis sets are reported for these hydrocarbons, based on experimental r_e distances. The measured gas phase ^{1}H chemical shifts have been converted to an absolute σ_0 shielding scale by use of the literature shielding of methane. These and gas phase ^{13}C literature values have been transferred with literature ZPV data to estimated σ_e^{exp} shieldings which are used to evaluate the basis set dependence of the calculated σ_e shieldings utilizing linear least squares regressions. Exponential extrapolations of Dunning basis set calculations allow the determination of basis set limits for ^{1}H and ^{13}C shieldings.

^{1}H and ^{13}C chemical shifts have been derived from the HF calculated shieldings with shieldings of TMS which has been geometry optimized and GIAO calculated in each basis. Standard deviations (*esd*) as low as 0.09 ppm for ^{1}H and 0.76 ppm for ^{13}C calculations have been obtained.

The statistically best basis set for simultaneous calculation of ^{1}H and ^{13}C absolute shieldings or relative shifts is 6-311G* within the HF and B3LYP methods. Aiming for highest accuracy and precision, ^{1}H and ^{13}C have to be treated separately. In this case, best results are obtained using MP2/6-311G** or higher for ^{1}H shieldings and MP2/cc-pVTZ for ^{13}C shieldings.

Key words: Experimental Gas Phase ^{1}H NMR Measurements, GIAO MO Calculations, Basis Set Dependence, ^{1}H and ^{13}C Absolute Shieldings and Chemical Shifts, Extrapolations with Dunning Basis Sets

Introduction

NMR spectroscopy is the most important analytical tool for determinations of molecular structures of organic molecules developed during the last 40 years [1 – 3].

Ab initio MO calculations of absolute chemical shieldings (σ) or chemical shifts (δ, based on reference to TMS) evolved during the last decades with large improvements of algorithms, programs and computer capacities as reviewed lately [4 – 6].

A basic problem is the selection of a gauge origin for the vector potential in the molecular electronic Hamiltonian which represents not uniquely the applied external magnetic field [7]. A first solution to the gauge problem was the use of *i*ndividual *g*auges for *l*ocalized molecular *o*rbitals (IGLO) by the group of Kutzelnigg [8, 9] and other approaches like LORG [10] or CSGT [11]. But the most widely used approach is termed GIAO from *g*auge *i*ncluding *a*tomic *o*rbitals. Such orbitals had been already suggested in 1937 by London for simple HMO calculations of magnetic susceptibilities [12, 13]. Later, Ditchfield introduced them into *ab initio* Hartree-Fock theory [14, 15] and since Pulay *et al.* [16] developed an efficient computer implementation in 1990, the GIAO method has become a standard for calculating NMR chemical shifts, installed in most quantum chemical *ab initio* programs like GAUSSIAN 98 [17], which we use here.

GIAO NMR calculations usually refer to isolated rigid molecules with fixed conformations at 0 K and are affected by the following aspects:

1. Selection of molecular geometries [18 – 20].
2. Extend and flexibility of basis sets [21 – 24].

3. Calculational procedures (a comparison of HF, DFT and MP2 methods is presented in ref. [23]), with the following aspects:
   a) The single-determinantal self-consistent field Hartree-Fock (HF) method [25] serves as the traditional standard type approach [19, 22, 23].
   b) This standard seems to be replaced lately by density functional theory (DFT) [26] which incorporates in formulations for the exchange-correlation functional some effects of electron correlation [22, 27 – 31].
   c) Post-Hartree-Fock methods: For very accurate calculations, post-HF methods for treatment of electron correlation are necessary as developed and reviewed lately by Gauss *et al.* [5].
   d) One approach for this is the many-body perturbation theory by Møller and Plesset [32] with perturbative treatment of higher excitations of second order as MP2 [33], third order as MP3 [34] and fourth order as MP4 [34].
   e) As most advanced treatment of electron correlation the coupled cluster (CC) theory has been introduced for single and double excitations (CCSD) [35, 36] and perturbative corrected triple excitations (CCSD(T)) [37].
   f) In multi-correlation SCF theory (MCSCF) [38] a linear combination of several Slater determinants is used.
4. Rovibrational and thermal effects [39 – 42] take care about the thermal occupation of rotational and vibrational levels from 0 K to the experimental measuring conditions around 300 K. These are not routinely calculated and available only lately, but necessary for accurate predictions of absolute shieldings.
5. Relativistic effects [43] are important for heavy atoms but not for hydrocarbons studied here.
6. Environmental effects [44] have to be considered if solution NMR spectra are used for comparison as well as pressure dependence [45, 46] for gas phase data.
7. For calculations of chemical shifts the standard TMS has to be calculated in a selected geometry (an experimental ED r_g structure is reported recently in ref. [47]) and with the same basis set as the considered molecule.

Most papers on GIAO NMR calculations concentrate on ^{13}C and heteroatom nuclei like ^{15}N, ^{17}O, ^{19}F, ^{29}Si and ^{31}P [22, 23, 27, 29, 31, 48, 49] but less so on ^{1}H spectra [21, 24, 28, 30, 50].

Benchmark type calculations for non-hydrogen NMR shieldings of small molecules using the advanced CI methods CCSD(T) [37] and CCSDT [51] with large basis sets lead to agreements in the range of experimental accuracy. This level cannot be extended to larger systems and with less advanced procedures deviations in the range of $\pm$5 ppm are obtained for ^{13}C and $\pm$1 ppm for ^{1}H.

Our aim in this paper is to evaluate the dependence of GIAO calculated ^{1}H and ^{13}C NMR shieldings and chemical shifts of seven hydrocarbons on different standard basis sets, independent on variations of the underlying molecular geometry, for which we selected experimental r_e distances. We used 25 basis sets on the HF level of theory, 16 for the hybrid DFT B3LYP method, and 12 for the MP2 approach.

For experimental ^{13}C values independent of solvation effects we used the gas phase data of ref. [46] (which are extrapolated to zero pressure) and own determinations of gas phase ^{1}H chemical shifts at atmospheric pressure.

The accuracy of calculated and experimental NMR values is studied statistically by linear least squares regressions, considering correlation coefficients, standard deviations and the slopes of the best fit straight lines.

Another question remains: Whether to regard relative chemical shifts based on TMS or absolute shieldings. Though former are the common result of NMR experiments, therefore being the natural choice for practical chemists who wish to use calculated values as reference or for prediction, only the latter can be obtained directly from *ab initio* calculations. The generation of relative shifts by subtraction from the additionally calculated shieldings of the TMS standard gives some benefit through error cancellation [27], but the effect is not very systematic and dependent on the applied TMS geometry [47]. Hence, good accuracy of the shielding values itself is a legitimate goal.

Since published gas phase NMR measurements of simple organic molecules are quite rare, we recorded ^{1}H NMR spectra at 400 MHz for all examined compounds. Here, attention was paid to obtain spectra at equilibrated temperature and atmospheric pressure. The sample and the reference substance TMS were measured together in a new, versatile usable flow probe with the flow NMR technique [52] as described in the experimental section.

Compound			r_{CH} [Å]		r_{CC} [Å]		α_{XCH} [°]	α_{CCC} [°]
Methane	**1**[a]		1.0862(12)				109.4712	
Ethane	**2**[b]		1.0877(50)		1.5280(30)	HCH	107.31(50)	
Ethene	**3**[c]		1.081(2)		1.334(2)	HCH	117.37(33)	
Ethyne	**4**[d]		1.0608		1.2031		180.0	
Propane	**5**[e,f]	C^1H'	1.0882(26)		1.5297(30)	C^2C^1H'	111.36	112.77
		C^1H''	1.0890(26)			C^2C^1H''	111.05	
		C^2H^2	1.0894(26)			$C^1C^2H^2$	109.38	
Butadiene	**6**[e,g]	C^1H^1	1.0805(26)	C^1C^2	1.3359(30)	$C^2C^1H^1$	121.55	123.89
		C^1H^2	1.0788(26)	C^2C^3	1.4723(30)	$C^2C^1H^2$	121.35	
		C^2H^3	1.0817(26)			$C^1C^2H^3$	116.58	
Benzene	**7**[h]		1.0802(20)		1.3914(10)		120.0	120.0

Table 1. Experimental and extrapolated molecular r_e distances and angles used for the NMR calculations (quoted error in parentheses).

[a] Ref. [57]; [b] ref. [58]; [c] ref. [59]; [d] ref. [60]; [e] extrapolated, error = two times esd; [f] H′ in CCC plane, H″ out of plane; [g] notations see Fig. 2; [h] ref. [61].

Selection of Molecules

For this work, the following seven small hydrocarbons were chosen: methane (**1**), ethane (**2**), ethene (**3**), ethyne (**4**), propane (**5**), s-*trans*-1,3-butadiene (**6**), and benzene (**7**). This selection comprises only a small section of hydrocarbons, yet it covers all possible hybridizations of carbon (sp^3, sp^2, sp), also in CH bonds, and the basic types of CC bonds – single, double, triple, and benzenoid. These selected molecules contain ten nonequivalent hydrogen nuclei and nine different carbon nuclei.

Selection of Molecular Geometries

Concerning the molecular geometry underlying the NMR calculations, one may pragmatically choose to optimize these with the same basis set as the one applied to the NMR calculation. Yet this implies a different geometry for each chemical shift calculation, making this approach inappropriate for a comparative study of basis set influences (the variation with molecular geometry [39, 40, 42] is of similar size as that with basis set and will be the topic of a separate publication). A better choice is to do the geometry optimization fully independent of the GIAO calculation using a post-HF method and a basis set large enough to deliver reliable r_e geometries.

We excluded this problem by using experimental distance parameters, and for consistency with calculated geometries, solely r_e distances, which are available only for few small molecules. r_e denotes an equilibrium distance at the minimum of the potential energy curve. Therefore, geometries calculated with quantum chemical methods by gradient optimization always deliver r_e distances, which are however strongly dependent on basis set [53, 54] and on calculational procedure [55, 56].

The experimental geometric parameters (atomic distances r_e and, if available, angles α_e) of molecules **1** to **4** and **7** were taken from the literature [57 – 61]. For each molecule, a plausible symmetry was assumed – T_d for **1**, D_{2d} for staggered **2**, D_{2h} for **3**, $D_{\infty h}$ for **4**, C_{2v} for staggered **5**, C_{2h} for **6** und D_{6h} for **7**.

For molecules **5** and **6**, no published experimental r_e geometries are available. To extend the statistical range, these distances were extrapolated using regression equations between experimental and calculated r_e distances from a previous work of our group [62]. Among the basis sets studied there and also covered by this work, 6-311++G** gives the statistically best correlation for CC distances with a correlation coefficient R of 0.99995 and a standard error of estimate (*esd*) of 0.0015 Å. The equation of this regression is: $r_{exp} = 0.9484 * r_{calc} + 0.0807$ Å. For CH bonds, the most favorable basis set is 6-311G** with $R = 0.99612$, $esd = 0.0013$ Å and the applied regression equation is: $r_{exp} = 0.8599 * r_{calc} + 0.1541$ Å.

The missing angles were obtained by geometry optimizations with distances constrained to the extrapolated values. All distances and angles used in this work are collected in Table 1.

Experimental Procedure

The experimental equipment for the investigation of gases and volatile liquids by flow ^{1}H NMR spectroscopy is depicted in Fig. 1. The apparatus consists of a 9.4 T Bruker ARX 400 NMR instrument (400 MHz proton resonance) equipped with a temperature and pressure stable flow probe with a 120 μl detection cell. The inlet and outlet of the probe are connected to a set of two Valco 6-port valves by stainless steel capillaries. With valve 1 it is possible to load the NMR flow cell with the samples and then seal it. TMS (b. p. 298 K) was used as internal reference standard; it was injected with a deep-frozen syringe *via* the loop at valve 2. Referencing on internal TMS at the same state of aggregation[a] as the sample was applied to avoid the susceptibility

[a] TMS is gaseous at the applied measuring conditions.

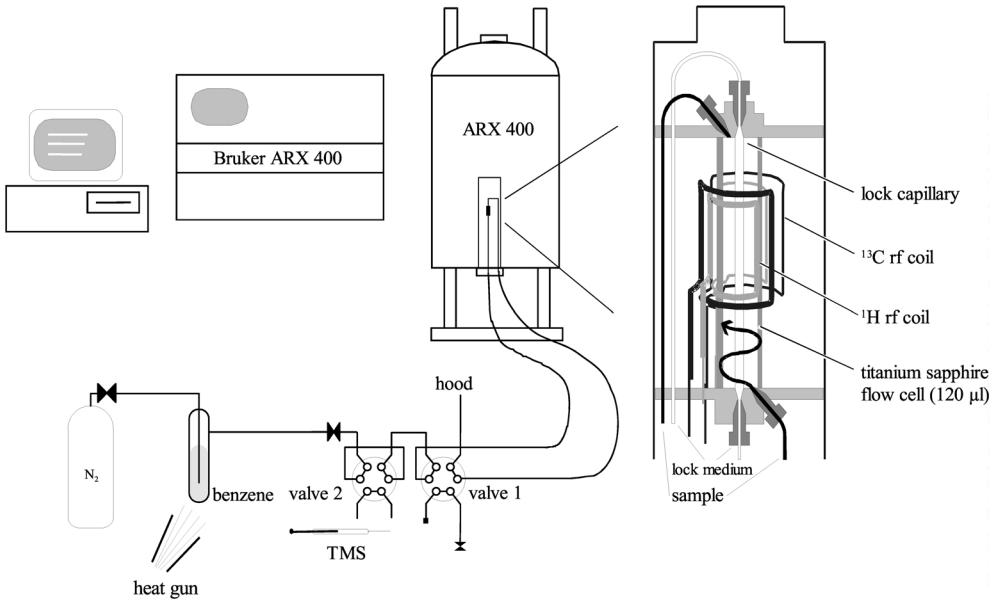

Fig. 1. Experimental set-up (left) with flow probe (right) for ^{1}H NMR measurements of gases and volatile liquids in the gaseous state.

corrections, which would be necessary when using external, soluted standards [2]. Without this, substantial differences in chemical shift (2 to 3 ppm high-field) are observed going from the liquid to the gaseous state due to the bulk susceptibility effect. Ahead of valve 2 the bottles with gaseous hydrocarbons (Compounds **1** to **6**)[b] or gaseous nitrogen for the volatile liquid benzene (**7**) are connected and the gases used as carrier to transport TMS to the NMR flow cell simultaneously. For **7**, a glass vessel is inserted between valve 2 and the nitrogen bottle. By heating the glass vessel with a heat gun it is possible to transport the sample vapor in the carrier gas stream to the NMR flow cell. The gas flow can be regulated with the valve of the gas cylinder. After loading the NMR flow cell with the gaseous sample, valve 1 is switched to the stop-flow position. At this time, the outlet of the NMR flow cell is open, leading to pressure compensation to atmospheric pressure. Following, the outlet is closed by a valve.

In the right part of Fig. 1 the NMR flow probe is shown. The main part is the pressure-stable titanium-sapphire flow cell holding the sample. Inside this tube, a small capillary for deuterated solvent is built in to work as lock chamber for field-frequency stabilizing. The advantage of this construction is that the lock solvent is spatially separated from the sample tube and therefore does not interact with the sample. The lock chamber was filled either with d_6-benzene or D_2O (for the measurement of benzene at elevated temperature). Shimming was done on the Fourier transformed spectrum. For each spectrum, one transient was acquired with 16k data points and a sweep width of 8064 Hz at 298 K for gaseous samples and 353 K for benzene, respectively.

With the described set-up it is possible to obtain ^{1}H NMR spectra of different compounds in a few minutes, simply by connecting and disconnecting the gas bottles ahead of valve 2. However, gas phase ^{13}C NMR spectra could not be obtained with this probe setting.

For the standard routine NMR experiments of dissolved substances, the pure gases **1** to **6** were introduced *via* a stainless steel needle into the solvent directly in the NMR tube for about two minutes. The solutions of gases and benzene (**7**) in $CDCl_3$ were measured on a Bruker AC 250 spectrometer at 297 K with TMS as internal standard.

Calculational Procedure and Selection of Basis Sets

The shielding constants – of both hydrogen and carbon atoms – of compounds **1 – 7** were calculated using the GIAO method implemented in the Gaussian 98 program suite [17], employing HF, MP2 and B3LYP procedures.

The majority of our calculations were performed in the single determinantal restricted Hartree-Fock model (HF) [25], employing a variety of altogether 17 of Pople's standard basis sets [63], namely minimal STO-3G and STO-6G, as well as split-valence 3-21G, 6-31G

[b] Compounds **1 – 3**, **5**, and **6** were obtained from Sigma-Aldrich Chemie GmbH as lecture bottles; **4** as a technical gas.

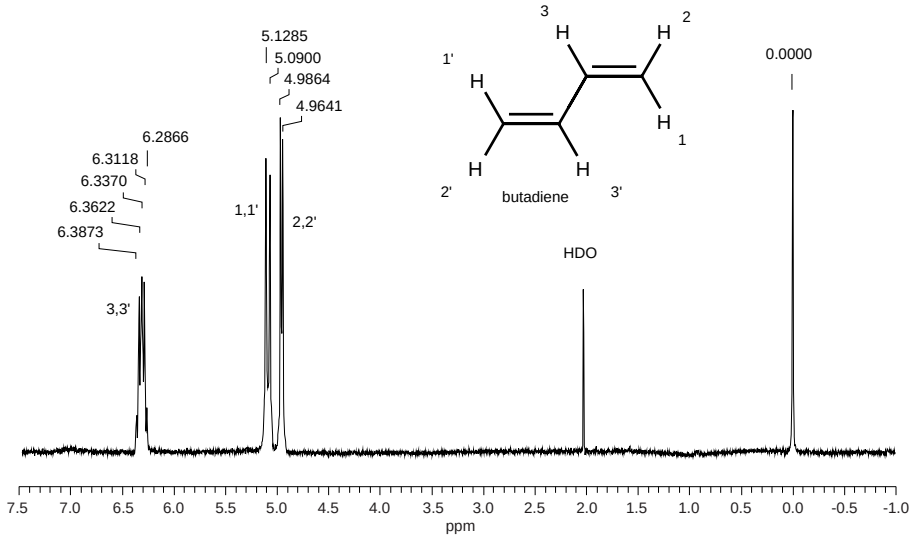

Fig. 2. Experimental ^{1}H NMR spectrum of gaseous butadiene referenced to internal TMS.

and 6-311G, the latter two also extended by all combinations of polarization (*) and diffuse (+) functions on carbon and additionally on hydrogen (**, ++). Furthermore, Dunning's correlation consistent polarized valence basis sets cc-pVnZ [64] were applied, with *n* (the number of zeta exponents) being 2 to 5 denoted by D, T, Q, and 5, both without and with augmentation by diffuse functions (denoted by aug).

To test whether HF is able to deliver NMR chemical shifts of sufficient quality in comparison to DFT and more expensive post-HF methods, we included the hybrid density functional method B3LYP (Becke's three-parameter functional with exact HF exchange and Lee-Yang-Parr exchange-correlation) [65, 66] in our survey, and also the MP2 approach [32], which is a perturbational approximation of second order for correlation effects. For these methods, only a smaller range of Pople's basis sets was employed, yet including the most important ones. Basis sets from the Dunning series were applied on the B3LYP level up to aug-cc-pV5Z, except for benzene, where limitations of the program prevented the last type of calculation. On the MP2 level, the largest accomplishable basis sets were[c] aug-cc-pVQZ for methane (**1**) and ethyne (**4**), cc-pVQZ for ethene (**3**), aug-cc-pVTZ for ethane (**2**), cc-pVTZ for propane (**5**), butadiene (**6**), and benzene (**7**).

[c]Gaussian 98 is limited to 2 GB main memory and 16 GB disk space on 32 bit systems, which allows even so-called "direct" MP2 calculations with larger basis sets only for the smallest molecules.

To gain chemical shifts, which are easier to compare with experimental data than absolute shieldings, the geometries and shieldings of tetramethylsilane (TMS) were calculated for all Pople basis sets on the HF level with results presented in Table 11. Of course, chemical shifts can only be generated from shieldings calculated with the same method and basis set.

Results and Discussion

Spectra and experimental shifts

Gas phase ^{1}H NMR spectra were determined in the way described above for all compounds studied. As an example of the quality of the spectra, Fig. 2 shows the spectrum of butadiene (**6**). Due to the smaller coupling constant of 9 Hz, the signal at 4.97 ppm was assigned to protons 2 and 2', and the signal at 5.11 ppm with a coupling constant of 15 Hz was assigned to protons 1 and 1'. The geminal coupling could not be resolved. Protons 3 and 3' appear around 6.35 ppm. Because the rules of first order are not valid for this spin-coupled spectrum, the real chemical shifts of the protons of butadiene have to be calculated by simulation. For this, we used the WIN-DAISY program of Bruker Daltonics, Bremen, Germany.

The simulated spectrum with iterated chemical shifts and coupling constants is shown in the lower part of Fig. 3 in comparison to the experimental spectrum in the upper trace. There, one may notice some shoulders not visible in Fig. 2. These appear on reprocessing the FID with zero-filling of 16 k points. For better fit-

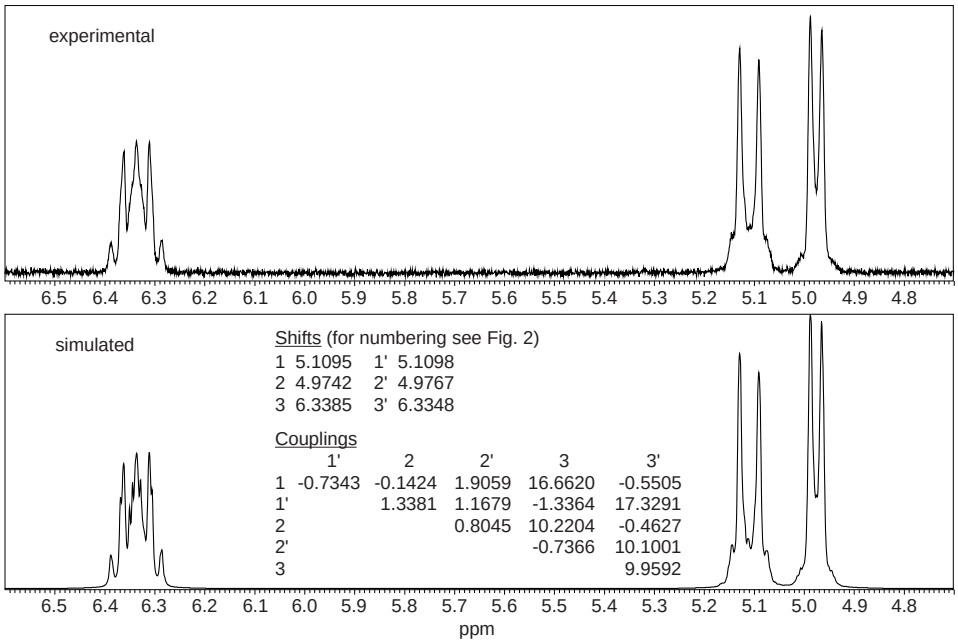

Fig. 3. Detail of experimental (above) and simulated (below) ^{1}H NMR spectra of butadiene by comparison. Indicated shifts and couplings as resulting from simulation.

Table 2. Experimental chemical shifts δ and absolute shieldings σ in the gas phase and chemical shifts in $CDCl_3$ solution for ^{1}H and ^{13}C (in ppm, shifts from TMS).

Compd.	Proton / Carbon	δ_H[a] [gas phase]	δ_H[b] [$CDCl_3$]	σ_C [gas phase]	δ_C [gas phase]	δ_C[c] [$CDCl_3$]
1		0.140	0.217	195.1[d]	−7.0[f]	−1.8[g]
2		0.880	0.856	180.9[d]	7.2[f]	6.69
3		5.308	5.406	64.5[d]	123.6[f]	122.96
4		1.458	1.909[a]	117.2[d]	70.9[f]	71.78 [h]
5	CH_3	0.929	0.898	170.8[e]	17.31[e]	16.21
	CH_2	1.377	1.327	169.1[e]	18.96[e]	16.46
6	H^2	4.975	5.109	–	–	–
	H^1 / C^1	5.110	5.222			117.51
	H^3 / C^2	6.337	6.347			137.71
7		7.236	7.344[a]	57.2[d]	130.9[f]	128.40[h]

[a] This work, 400 MHz; [b] this work, 250 MHz; [c] this work, 62.5 MHz; [d] ref. [46]; [e] calculated from ref. [85]; [f] calculated from ref. [46]; [g] ref. [86], in cyclohexane, there referenced to benzene, which is given as 129 ppm downfield from TMS; [h] this work, 100 Mhz.

ting, the simulation was carried out assuming a six-spin system. The resulting chemical shifts were averaged in pairs of X and X'.

In Table 2 all available experimental ^{1}H and ^{13}C chemical shifts in the gas phase and in $CDCl_3$ solution are summarized, both own measurements and literature values.

Gas phase ^{1}H chemical shifts and $CDCl_3$ solution values are linearly correlated by the equation $\delta_{gas} = 0.9945 * \delta_{solut} - 0.070$ with $R = 0.9985$ and an *esd* of 0.152 ppm. The corresponding ^{13}C regression equation is $\delta_{gas} = 1.0172 * \delta_{solut} - 0.646$ with $R = 0.9992$ and an *esd* of 2.502 ppm.

Absolute shieldings of hydrogen

The absolute ^{1}H shieldings for all of our calculations are plotted in Fig. 4. These graphs show clearly a strong basis set dependence. Individual values per proton vary up to 2.5 ppm, but the changes with basis sets are rather similar for all protons.

Minimal and simple split-valence Pople basis sets show largest numerical values which decrease in steps on inclusion of polarization functions on carbon (one star) and on hydrogen (two stars). The addition of diffuse functions shows only a negligible small effect. The numerical decrease from the 6-31G series to the 6-311G series is also rather small.

A downward trend of shieldings is also apparent for the Dunning basis set series with increasing basis set size, for HF as well as on the MP2 and B3LYP levels. Diffuse functions (augmented Dunning basis sets) have also only a small effect.

Till now, of our seven molecules only for methane an experimental gas phase shielding value of 30.611 ± 0.024 ppm has been reported [67]. This value is used

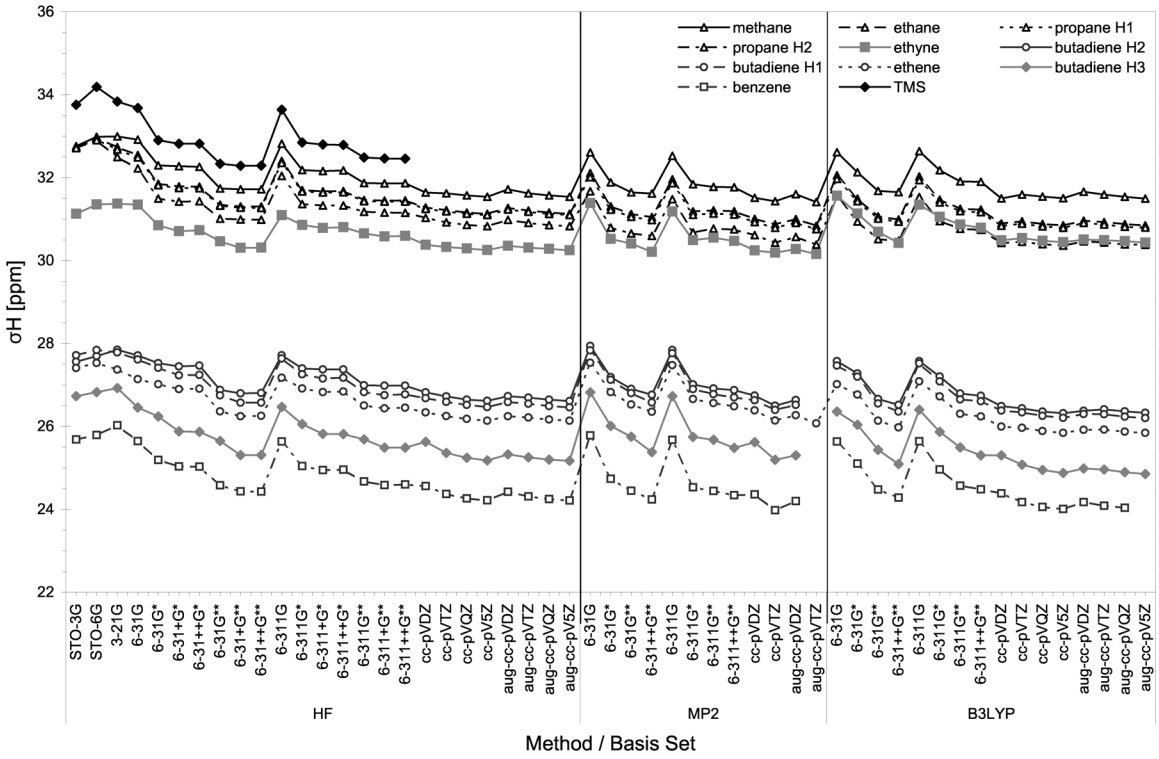

Fig. 4. Calculated absolute shieldings of hydrogen (σ_e^H in ppm) of molecules **1 – 7** for 25 basis sets for the HF, 12 for the MP2, and 16 for the B3LYP method.

in Table 3 to convert our experimental gas phase shifts of Table 2 to an experimental absolute shielding scale. (It should be noted that our experimental shifts are not extrapolated to zero pressure and the measuring temperature was not controlled. However, our methane related data are very close to some published gas phase values shown in the fifth column of Table 3.) These shielding values are denoted as σ_0, referring to real gaseous molecules which are vibrating and rotating at 300 K. Our calculations on the other hand refer to frozen molecules at 0 K in fixed conformations defined by the selected r_e geometries and therefore deliver shielding values which we designate as σ_e. For accurate comparisons all calculated σ_e shieldings should be corrected for internal motional effects leading then to calculated σ_0 values.

Alternatively other kinds of experimental molecular distances [68] could be used. For example for methane (**1**), our selected experimental CH r_e distance is 1.0862(12) Å [57]. The MW r_z value 1.0995(12) Å [69] and the ED r_α^0 value 1.0987(12) Å [69] both refer physically to the same zero point vibrational level (MW = microwave spectrum, ED = electron diffraction). The ED r_g distance of 1.1040(4) Å [70] is defined as a thermal average about partially excited vibrational and rotational levels. These values indicate the strong anharmonicity of the CH potential energy curve leading to elongation from the minimum r_e value with thermal excitations.

It is known [71] that an increase of CH distances leads to a decrease of calculated shieldings. Therefore the use of the larger r_g or r_z distances instead of the smaller r_e values should yield better calculated shielding values for direct comparison with experimental σ_0 values.

We discarded both of these approaches: the first one because the effort of correcting each performed calculation for rovibration would be much too large and the second one because it introduces a geometry dependence which we just wanted to eliminate.

We decided to correct our experimental σ_0 values by use of the zero-point vibrational (ZPV) corrections from recent calculations by Ruud *et al.* [42] to derive

Table 3. Adjustment of our experimental gas phase chemical shifts (δ_{TMS}) of Table 2 to absolute shieldings (σ_0) based on the methane value from [67] and application of zero point vibration corrections ($\Delta\sigma_{ZPV}$) from [42] to σ_e^{exp} values

Compd.	Group	δ_{TMS}	σ_0	lit. σ_0	$\Delta\sigma_{ZPV}$[b]	σ_e^{exp}	σ_e^{calc} [b]
1		0.136	30.611[a]	30.611 (24)[a]	0.59	31.201	31.96 31.60[f] 31.26[g]
2		0.882	29.865	29.870[c]	0.67	30.535	31.52
3		5.308	25.439	25.430[c]	0.52	25.959	26.80
4		1.458	29.289	29.276[c] 29.278[d]	0.76	30.049	30.98
5	C^1H'	0.929	29.818		0.69	30.508	31.34
	C^1H''						31.60
	C^2H	1.377	29.370		0.70	30.070	31.21
6	H^1	5.110	25.637		0.42	26.057	27.03
	H^2	4.975	25.772		0.47	26.242	27.20
	H^3	6.337	24.410		0.54	24.950	25.85
7		7.236	23.512	23.57[e]	0.38	23.892	24.81 24.20[h] 23.2 to 24.3[e,i]

[a] Ref. [67]; [b] ref. [42]; [c] ref. [87]; [d] ref. [88]; [e] ref. [89]; [f] ref. [37], CCSD(T) result; [g] ref. [38], MCSCF result; [h] ref. [16]; [i] estimated HF limit.

estimated experimental shieldings (denoted as σ_e^{exp}) presented in Table 3.

Methane (**1**) as the prototype of saturated hydrocarbons may be used as secondary standard as done with the value of 30.611 ppm to derive experimental absolute shieldings σ_0 in Table 3. Due to its small size its shielding can be calculated with very advanced methods. Several results of GIAO benchmark calculations for r_e distances with very large basis sets have been presented by Gauss and Stanton [5, 37]: for r_e geometry, the HF limit σ_e is 31.7 ppm, the MP2 shielding is 31.4 ppm, which increases to 31.5 ppm in MP3, MP4 and CCSD calculations. The most advanced calculations yield 31.60 ppm with CCSD(T) and 31.26 ppm with MCSCF [38], but this with a larger CH distance of 1.094 Å. These values show a small dependence on calculational procedures and nearly no influence of electron correlation. Our estimated σ_e^{exp} shielding of 31.20 ppm is close to these values, and in much better agreement than the experimental σ_0 of 30.611 ± 0.024 ppm.

The last column in Table 3 lists HF calculations from ref. [42] using a triple zeta basis with polarization functions on C and H. The methane value of 31.96 ppm is larger than the before mentioned values. Our smallest calculated σ_e values for methane with largest basis sets are 31.54 ppm on the HF, 31.41 ppm on the MP2, and 31.50 ppm on the B3LYP level.

Extrapolations of Dunning basis set calculations for ^{1}H shieldings

The consecutive character of Dunning's correlation consistent basis sets [64, 72] which all include polarization functions allows an exponential extrapolation for the determination of the corresponding basis set limit. This procedure was suggested by Feller [73] and applied for the Hartree-Fock limit of energies [73, 74] and for estimation of experimental r_e distances [75, 76].

Our calculated Dunning values have been extrapolated to the limit by use of the equation $\sigma = \sigma_{limit} + be^{-k\zeta}$ for at least three consecutive values. The parameter σ_{limit} delivers the basis set limit shielding. In Table 4, our extrapolated limits for the molecules **1**–**7** are presented together with deviations $\Delta\sigma_e$ from the estimated σ_e^{exp} values.

Table 4. Exponentially determined Dunning basis set limits (σ_{limit}) for ^{1}H shieldings ($\Delta\sigma_e$ are deviations from σ_e^{exp} shieldings of Table 3).

		HF		HF aug		MP2		MP2 aug		B3LYP		B3LYP aug	
Compd.		σ_{limit}	$\Delta\sigma_e$	σ_{limit}	$\Delta\sigma_e$	σ_{limit}	$\Delta\sigma_e$	σ_{limit}	$\Delta\sigma_e$	σ_{limit}	$\Delta\sigma_e$	σ_{limit}	$\Delta\sigma_e$
1		31.506	0.305	31.510	0.309	[a]		31.193	−0.008	31.470	0.269	31.342	0.141
2		31.011	0.476	31.051	0.515					30.802	0.267	30.820	0.285
3		26.028	0.068	26.079	0.120	25.686	−0.273			25.777	−0.183	25.780	−0.179
4		30.150	0.101	30.078	0.029	[a]		29.889	−0.160	30.380	0.331	[a]	
5	H^1	30.974	0.465	30.983	0.475					30.758	0.249	30.787	0.279
	H^2	30.792	0.721	30.768	0.698					30.326	0.255	30.375	0.305
6	H^1	26.300	0.242	26.431	0.373					26.122	0.065	26.175	0.118
	H^2	26.549	0.307	26.559	0.316					26.292	0.049	26.271	0.028
	H^3	25.132	0.182	25.106	0.156					24.791	−0.160	24.786	−0.164
7		24.162	0.270	24.173	0.281					23.948	0.057	23.977	0.086
av. $\lvert\Delta\sigma_e\rvert$			0.314		0.327		0.273		0.084		0.188		0.176
av. $\lvert\Delta\sigma_0\rvert$ [b]			0.888		0.901		0.247		0.591		0.694		0.653

[a] Calculated shieldings could not be fitted by exponential function; [b] average deviations from experimental σ_0 shieldings of Table 3.

	Basis set	av. $\Delta\sigma_0$ [ppm]	Rank	av. $\Delta\sigma_e$ [ppm]	Rank	R	Rank	esd [ppm]	Rank	m	Rank	b [ppm]	Rank
HF	STO-3G	2.344		1.770		0.98828		0.447		0.9299		0.314	
	STO-6G	2.508		1.934		0.98895		0.434		0.9151		0.601	
	3-21G	2.451		1.877		0.99205		0.369		0.9610		−0.714	
	6-31G	2.237		1.663		0.99543		0.280		0.9396		*0.126*	*1*
	6-31G*	1.798		1.224		0.99777		0.195		1.0096	3	−1.503	
	6-31+G*	1.672		1.098		0.99738		0.212		0.9859		−0.689	
	6-31++G*	1.675		1.101		0.99744		0.209		0.9867		−0.715	
	6-31G**	1.238		0.664		0.99813		0.179		0.9860		−0.263	3
	6-31+G**	1.123		0.549		0.99769		0.199		0.9619		0.536	
	6-31++G**	1.124		0.550		0.99776		0.196		0.9626		0.516	
	6-311G	2.162		1.588		0.99499		0.293		0.9665		−0.598	
	6-311G*	1.672		1.098		*0.99872*	*1*	*0.148*	*1*	1.0047	1	−1.235	
	6-311+G*	1.598		1.024		0.99839	5	0.166	5	0.9884	4	−0.689	
	6-311++G*	1.606		1.032		0.99846	3	0.163	3	0.9884	5	−0.696	
	6-311G**	1.357		0.783		0.99847	2	0.162	2	0.9776		−0.139	2
	6-311+G**	1.300		0.726		0.99823		0.174		0.9637		0.315	
	6-311++G**	1.305		0.731		0.99830		0.171		0.9648		0.278	5
	cc-pVDZ	1.189		0.615		0.99765		0.201		0.9909	2	−0.353	
	cc-pVTZ	1.085		0.511		0.99824		0.174		0.9725		0.271	4
	cc-pVQZ	1.015	4	0.441	4	0.99840	4	0.166	4	0.9658		0.529	
	cc-pV5Z	0.975	2	0.401	2	0.99835		0.168		0.9630		0.648	
	extrapol. σ_e [a]			0.314		0.99823		0.174		0.9627		0.739	
	extrapol. σ_0 [a]	0.888				0.99808		0.174		0.9248		1.239	
	aug-cc-pVDZ	1.115		0.541		0.99812		0.179		0.9639		0.486	
	aug-cc-pVTZ	1.053	5	0.479	5	0.99825		0.173		0.9638		0.551	
	aug-cc-pVQZ	1.002	3	0.428	3	0.99837		0.167		0.9625		0.636	
	aug-cc-pV5Z	*0.972*	*1*	*0.398*	*1*	0.99834		0.169		0.9621		0.676	
	extrapol. σ_e [a]			0.327		0.99793		0.188		0.9675		0.592	
	extrapol. σ_0 [a]	0.901				0.99809		0.174		0.9296		1.089	

Table 5. Statistical parameters of linear regressions for HF calculated ^{1}H shieldings versus ZPV corrected experimental values σ_e^{exp} (10 data points for protons of **1** – **7**).

[a] Regressions with shieldings obtained from extrapolation of Dunning basis sets collected in Table 4.

For methane (**1**) the HF limit shieldings σ_e with 31.506 ppm and 31.510 ppm without and with diffuse functions are now very close to the benchmark calculation of 31.7 ppm [5]. Correlation effects are small for this molecule, and our extrapolated MP2 value of 31.19 ppm is close to the MP2 value of 31.40 ppm given in ref. [5] and in agreement to the MCSCF value of 31.26 ppm. The B3LYP limits of 31.47 ppm and 31.34 ppm are between these values.

The average deviations (av. $|\Delta\sigma_e|$) in Table 4 for all compounds show the same trend: largest values with 0.33 ppm for HF, smallest with 0.08 ppm for MP2 in the reverse direction, and B3LYP intermediate with 0.18 ppm. These deviations from estimated σ_e^{exp} values are definitely smaller than those based on experimental σ_0 shieldings. The inclusion of diffuse functions (augmented) increases deviations in the HF method but reduces these for B3LYP shieldings.

Due to limitations in computer facilities (see footnote c above), MP2 calculations with at least three consecutive Dunning basis sets for extrapolation could only be performed for molecules **1**, **3,** and **4**. The non-augmented MP2 sequence of shieldings of **1** and **4** as well as the augmented B3LYP series of **4** could not be fitted exponentially.

Linear regressions for ^{1}H shieldings

All our calculated r_e based shieldings (σ_e^{calc})[d] are for each basis set and each method larger than either experimental σ_0 or estimated σ_e^{exp} values of Table 3. Average deviations from these values are presented in Tables 5 and 6 as one-parameter descriptors of accuracy. The σ_e^{exp} based deviations ($\Delta\sigma_e$) are all smaller than σ_0 based deviations ($\Delta\sigma_0$) by a factor around two. For the HF calculations of Table 5, in the 6-31G and 6-311G families of basis sets these deviations decrease with the extension of basis functions with a smallest optimum value for the 6-31+G** calculations followed next by the 6-311+G** calculations.

The Dunning series show a steady decrease of deviations in the polarized and augmented families. The average deviations of the extrapolated shieldings fit well

[d] All calculated individual values may be obtained as supplementary material (Tables S1 to S10) at http://www.uni-tuebingen.de/uni/coh → Publications.

	Basis set	av. $\Delta\sigma_0$ [ppm]	Rank	av. $\Delta\sigma_e$ [ppm]	Rank	R	Rank	esd [ppm]	Rank	m	Rank	b [ppm]	Rank
MP2	6-31G	2.197		1.623		0.99932		0.108		1.0596		−3.384	
	6-31G*	1.391		0.817		0.99891		0.137		1.0495		−2.241	
	6-31G**	1.160		0.586		0.99927		0.112		1.0281		−1.387	
	6-31++G**	1.003	3	0.429	3	0.99916		0.120		*0.9982*	*1*	−0.378	4
	6-311G	2.078		1.504		0.99922		0.115		1.0717		−3.616	
	6-311G*	1.243		0.669		0.99943	5	0.099	5	1.0252		−1.389	
	6-311G**	1.210		0.636		*0.99962*	*1*	*0.080*	*1*	1.0043	2	−0.760	5
	6-311++G**	1.146	5	0.572	5	0.99955	4	0.088	4	0.9893	4	−0.266	3
	cc-pVDZ	1.033	4	0.459	4	0.99914		0.122		1.0254		−1.181	
	cc-pVTZ	*0.821*	*1*	*0.247*	*1*	0.99958	3	0.085	3	0.9868	5	0.127	2
	aug-cc-pVDZ	0.956	2	0.382	2	0.99958	2	0.084	2	0.9902	3	*−0.105*	*1*
	aug-cc-pVTZ[b]	0.871	–	0.216	–	0.99926	–	0.081	–	0.9729	-	0.596	–
B3LYP	6-31G	2.009		1.435		0.99808		0.182		0.9916	4	−1.187	
	6-31G*	1.580		1.006		0.99922		0.116		1.0239		−1.697	
	6-31G**	1.051		0.477		0.99907		0.126		0.9886	5	*−0.152*	*1*
	6-31++G**	0.899		0.325		0.99926		0.113		0.9660		0.637	5
	6-311G	1.998		1.424		0.99839		0.166		1.0065	3	−1.617	
	6-311G*	1.518		0.944		*0.99953*	*1*	*0.090*	*1*	*1.0038*	*1*	−1.055	
	6-311G**	1.207		0.633		0.99934		0.106		0.9705		0.211	3
	6-311++G**	1.149		0.575		0.99934		0.106		0.9589		0.597	4
	cc-pVDZ	0.898		0.324		0.99904		0.128		0.9942	2	−0.159	2
	cc-pVTZ	0.870		0.296		0.99941		0.100		0.9603		0.826	
	cc-pVQZ	0.791	3	0.231	3	0.99945	3	0.097	3	0.9530		1.106	
	cc-pV5Z	*0.748*	*1*	*0.211*	*1*	0.99944	4	0.098	4	0.9503		1.223	
	extrapol. σ_e[c]			0.188		0.99942		0.100		0.9458		1.401	
	extrapol. σ_0[c]	0.694				0.99924		0.110		0.9085		1.875	
	aug-cc-pVDZ	0.854	5	0.288	5	0.99927		0.112		0.9492		1.153	
	aug-cc-pVTZ	0.827	4	0.260	4	0.99947	2	0.096	2	0.9514		1.118	
	aug-cc-pVQZ	0.777	2	0.231	2	0.99943	5	0.099	5	0.9501		1.200	
	aug-cc-pV5Z[a]	0.776	–	0.227	–	0.99954	–	0.082	–	0.9370	–	1.621	–
	extrapol. σ_e[c]			0.176		0.99913		0.126		0.9534		1.195	
	extrapol. σ_0[c]	0.653				0.99905		0.127		0.9194		1.589	

Table 6. Statistical parameters of linear regression for MP2 and B3LYP calculated ^{1}H shieldings versus ZPV corrected experimental values σ_e^{exp} (10 data points except where noted).

[a] 9 data points; [b] 6 data points; [c] regressions with shieldings obtained from extrapolation of Dunning basis sets collected in Table 4.

into the sequence with absolutely smallest deviations around 0.31 ppm.

Corresponding deviations of shieldings from MP2 and B3LYP methods for a smaller selection of basis sets are shown in Table 6. They are in each case smaller than HF for the MP2 calculations and intermediate for B3LYP. The average deviations for DFT Dunning extrapolated shieldings are now only 0.18 ppm.

The basis set dependence may be studied quantitatively by means of linear least squares regressions of the form $\sigma_e^{exp} = m * \sigma_e^{calc} + b$. Statistical parameters for our σ_e^{exp} shieldings with all calculated shieldings are collected in Table 5 for HF and in Table 6 for MP2 and DFT B3LYP methods.

The correlation coefficient *R* and the standard error of estimate *esd* are both indicators of precision, while slope *m* and intercept *b* indicate the accuracy [77]. Precision means the conformity of the considered sample with a certain rule, not necessarily the correct one. Accuracy is the correctness of the sample, the closeness to the true value. As we premise the validity of the GIAO approach, the precision will indicate the ability of the specific model, that is, method and basis set, to give equally correct descriptions of the electron distribution (originating the shielding) of all molecules. This means, precision indicators will vary little and generally show good values except for the smallest basis sets. The major criterion of quality has to be the accuracy, here the closeness of the slope to one and of the intercept to zero. We put emphasis on the slope since a slope close to one leads to shift predictions of at least uniform quality over the whole interval of definition. Only then, the intercept may be considered as an incremental constant correction. Combined with a non-ideal slope, even a small intercept does not imply small deviations within the range of interest, as the point of origin may be far outside of this interval (this is especially true for absolute shieldings, where the zero point is defined as the bare nucleus, a state not available to experiment).

R values are poor for the first three basis sets of the HF values of Table 5 which will be safely discarded. Other *R* values are statistically highly acceptable in the range of 0.995 to 0.998. Standard deviations (*esd*) are between 0.293 and 0.148 ppm indicating high precision for a total range of about 13 ppm for the ^{1}H NMR scale. Best *R* and *esd* values delivers the 6-311G* basis set. In Table 6, best *R* and *esd* values (which behave always similar) are observed for the B3LYP calculations also with the 6-311G* basis set with $R = 0.9995$ and $esd = 0.090$ ppm. But corresponding MP2 parameters are best for the 6-311G** basis set with $R = 0.9996$ and $esd = 0.080$ ppm. The MP2 regressions for the augmented cc-pVTZ basis set cannot be compared quantitatively because they are based on a smaller number of data points. The tables contain rankings for the five best values of each parameter within one method.

Slopes and intercepts as indicators of accuracy improve for same basis sets on different levels of theory in the sequence HF < B3LYP < MP2, but the two parameters do not follow the same ranking pattern. The intercept is also best for 6-311G* HF and B3LYP calculations, but the MP2 intercept is most accurate for 6-31++G** which represents larger flexibility, but is better than that of the larger 6-311++G** basis set. Slopes show a different ranking as compared to *esd* which will not be discussed in detail.

Absolute shieldings of carbon

We could not measure gas phase ^{13}C NMR spectra with our installation, but experimental gaseous ^{13}C shielding values at 300 K (σ_0) extrapolated to zero pressure are available from ref. [46] as shown in Table 2 for all of our compounds except butadiene (**6**). As before in the case of ^{1}H shieldings, we have to differentiate between these experimental σ_0 values and calculated absolute shieldings σ_e^{calc} based on r_e geometries. In Table 7, we apply ZPV corrections from ref. [42] in a range of 3.2 to 5.9 ppm to derive corrected σ_e^{exp} values which may be compared directly to our calculated σ_e^{calc} values.

Methane

The simplest hydrocarbon methane (**1**) was treated in numerous calculations and it is important as a secondary standard for an absolute ^{13}C shielding scale. Its experimental σ_0 value is reported as 193.697 ppm in ref. [39], but as 195.1 ppm in ref. [46] and most recent as 194.8 ± 0.9 ppm in ref. [78]. In Table 7, three available ZPV values are given for the conversion from σ_0 to an estimated σ_e: From ref. [39] the total correction to nuclear motion at 300 K is calculated as 3.695 ppm and solely the smaller ZPV correction as 3.591 ppm. These are larger than the value of 3.20 ppm reported by Ruud *et al.* [42]. However, Ruud's ZPV values have been used in Table 7 to derive the estimated σ_e^{exp} values from the σ_0 data of the Jamesons [46]. Our value of 198.30 ppm is consistent to 197.374 ppm and the estimate of 198.5 ± 0.9 ppm of ref. [39]. Cited σ_e calculations for **1** in the last column of Table 7 are in very good agreement with these estimates. Most important is the CCSD(T) benchmark calculation of Gauss and Stanton [37] with 198.9 ppm which differs strictly from their σ_e HF limit value of 194.8 ppm. This difference shows the influence of electron correlation on ^{13}C shielding[e] which is more important than in the ^{1}H shieldings studied before.

Table 7. Zero point vibration corrections ($\Delta\sigma_{ZPV}$) of experimental ^{13}C gas phase shieldings (σ_0^{exp}).

Compd.		σ_0^{exp} [a]	$\Delta\sigma_{ZPV}$ [b]	σ_e^{exp}	σ_e^{calc} [b]
1		195.1	3.20	198.30	197.83
		193.697 [c]	3.591 [c]	197.374 [c]	197.392 [k]
		194.8(9) [d]	3.695 [c,h]	198.5(9) [c,f]	198.9 [i,m]
					194.8 [i,n]
2		180.9	3.95	184.85	186.61
		180.827(6) [e]			
3		64.5	4.79	69.29	65.68
		64.344(15) [e,f]			
4		117.2	4.44	121.64	120.03
		116.58(90) [g]			
5	C^1	170.8	4.26	175.06	178.65
		170.654(6) [e,f]			
	C^2	169.1	5.22	174.32	177.84
		169.069(6) [e,f]			
6	C^1		5.92		72.98
	C^2		4.13		50.26
7		57.2	3.37	60.57	59.46
					60.4 [o]
					57.73 [p]

[a] Ref. [46]; [b] ref. [42]; [c] ref. [39]; [d] ref. [78]; [e] ref. [90]; [f] based on methane = 194.8 ± 0.9 ppm (ref. [78]); [g] ref. [88]; [h] total correction to nuclear motions at 300 K; [i] ref. [37]; [k] ref. [79]; [m] CCSD(T) value; [n] estimated HF limit; [o] ref. [91], IGLO value; [p] ref. [16].

Other calculations for **1** are very nonuniform. Lazzeretti *et al.* [79] cite a compilation of 11 refer-

[e] In the recent review [5], large basis set calculations for r_e distances of **1** are reported with the following σ_e values: MP2: 201.0, MP3: 198.8, MP4: 199.5, CCSD: 198.7, MCSCF: 198.2 and CCSD(T): 199.1 ppm (the last value is in numerical discrepancy to 198.9 ppm given in ref. [37]).

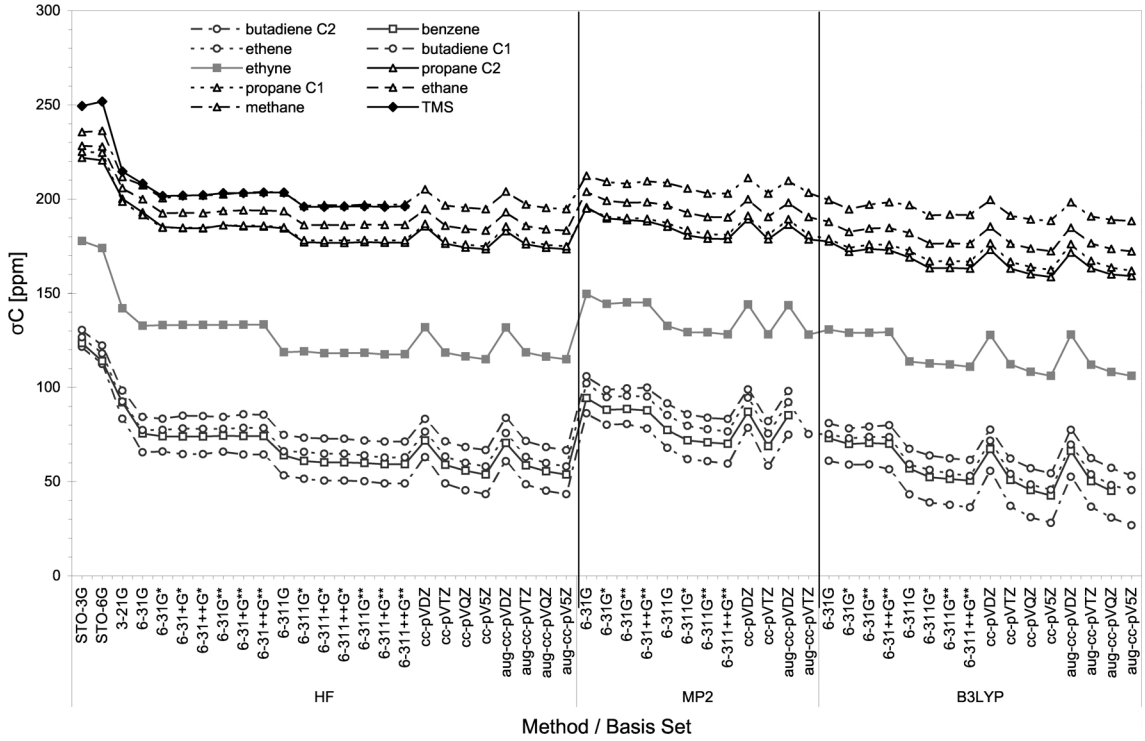

Fig. 5. Calculated absolute shieldings of carbon (σ_e^C in ppm) of molecules **1** – **7** for all employed methods and basis sets.

ences yielding shieldings between 172.6 and 239 ppm for **1**. Allen *et al.* [21] studied the dependence on 11 basis sets and obtained values between 197.1 and 211.9 ppm. Our HF calculations delivered σ_e values for methane between 194.7 and 236.2 ppm. DFT calculations for **1** cited in ref. [5] lead to the following values: DFT (BLYP) 184.3 ppm [80], CDFT (BLYP+VRG) 182.9 ppm [80], SOS-DFPT (BPW91) 191.2 ppm [49] and GGA DFT (modified B3LYP) 198.9 ppm [81]. This last value is in full agreement to the benchmark CCSD(T) calculation given above.

Other compounds

Experimental σ_0 values of ref. [46] are close to a few other gas phase determinations listed in the second column of Table 7. The average deviation of these to calculated σ_e values of ref. [42] is 4.47 ppm. However, our ZPV corrected estimated σ_e^{exp} shieldings are closer to the calculated σ_e values with an average deviation of 1.74 ppm.

The results of all our ^{13}C shielding calculations are shown graphically in Fig. 5. In the HF method, the basis set dependence is different for saturated and unsaturated carbon shieldings. Introduction of polarization functions (*) lowers the shieldings in the first case, but shows a negligible small effect for unsaturated carbon atoms. The ^{13}C shieldings are hardly influenced by additional polarization functions on hydrogen just as little as by diffuse functions. Similar to the ^{1}H shieldings, MP2 and B3LYP show parallel behavior for all types of carbon: a distinct step for the introduction of polarization at carbon with small change through the 6-31G family but clearly a lowering of shieldings with increase of functions in the 6-311G family. This shows the importance of flexibility in basis sets for post-Hartree-Fock calculations of ^{13}C shieldings.

Extrapolations of Dunning basis set calculations for ^{13}C shieldings

The basis set limits of exponential extrapolations of the Dunning basis set series for ^{13}C shieldings are presented in Table 8. The HF limit values for methane with 194.71 ppm and 194.52 ppm without and with diffuse functions, respectively, are very close to the HF bench-

Table 8. Exponentially determined Dunning basis set limits (σ_{limit}) for ^{13}C shieldings ($\Delta\sigma_e$ are deviations from σ_e^{exp} shieldings of Table 7).

Compd.		HF		HF aug		MP2		MP2 aug		B3LYP		B3LYP aug	
		σ_{limit}	$\Delta\sigma_e$	σ_{limit}	$\Delta\sigma_e$	σ_{limit}	$\Delta\sigma_e$	σ_{limit}	$\Delta\sigma_e$	σ_{limit}	$\Delta\sigma_e$	σ_{limit}	$\Delta\sigma_e$
1		194.707	−3.593	194.521	−3.779	201.163	2.863	200.502	2.202	188.383	−9.917	188.223	−10.077
2		183.365	−1.485	183.197	−1.653					172.123	−12.727	171.557	−13.293
3		57.843	−11.447	57.778	−11.512	69.674	0.384			44.694	−24.596	44.266	−25.024
4		114.906	−6.734	115.119	−6.521	124.525	2.885	124.397	2.757	105.840	−15.800	105.999	−15.641
5	C1	175.016	−0.034	174.821	−0.229					162.002	−13.048	160.846	−14.204
	C2	173.407	−0.953	173.246	−1.114					158.164	−16.196	158.458	−15.902
6	C1	66.478	1.568 [a]	66.438	1.528 [a]					53.343	−11.567 [a]	51.230	−13.680 [a]
	C2	43.069	−1.551 [a]	42.975	−1.645 [a]					27.088	−17.532 [a]	24.751	−19.869 [a]
7		53.613	−6.957	53.462	−7.108					41.539	−19.031	42.596	−17.974
av. $\lvert\Delta\sigma_e\rvert$			4.458		4.559		2.044		2.479		15.902		16.016
av. $\lvert\Delta\sigma_0\rvert$			3.413		3.365		6.187		6.299		11.726		11.841

[a] Derived from estimated experimental shieldings (see page 1166) and not included in average values.

	Basis set	av. $\lvert\Delta\sigma_0\rvert$ [ppm]	Rank	av. $\lvert\Delta\sigma_e\rvert$ [ppm]	Rank	R	Rank	esd [ppm]	Rank	m	Rank	b [ppm]	Rank
HF	STO-3G	54.884		50.708		0.99754		4.372		1.1607		−81.449	
	STO-6G	51.508		47.332		0.99763		4.291		1.0714		−60.743	
	3-21G	26.887		22.711		0.99676		5.016		1.0571		−32.032	
	6-31G	17.527		13.352		0.99788		4.064		0.9754	4	−9.572	
	6-31G*	13.294		9.119		0.99853		3.387		1.0350		−14.358	
	6-31+G*	13.520		9.345		0.99908		2.670		1.0344		−14.509	
	6-31++G*	13.450		9.275		0.99909		2.661		1.0345		−14.438	
	6-31G**	14.203		10.027		0.99883		3.017		1.0258		−13.906	
	6-31+G**	14.337		10.162		0.99923		2.450		1.0251		−13.950	
	6-31++G**	14.337		10.161		0.99928		2.374		1.0249	5	−13.920	
	6-311G	8.663		6.249		0.99781		4.128		0.9294		5.752	5
	6-311G*	4.146		*2.219*	*1*	0.99920		2.495		0.9774	3	*3.204*	*1*
	6-311+G*	3.793		2.389	3	0.99920		2.503		0.9693		4.684	3
	6-311++G*	3.742		2.347	2	0.99919		2.513		0.9708		4.530	2
	6-311G**	3.922		2.570		0.99916		2.561		0.9640		5.431	4
	6-311+G**	3.756		2.885		0.99907		2.698		0.9580		6.770	
	6-311++G**	3.798		2.838		0.99910		2.646		0.9578		6.733	
	cc-pVDZ	13.993		9.817		0.99940	3	2.154	3	*0.9982*	*1*	−9.543	
	cc-pVTZ	3.542	5	2.561	5	0.99931		2.312		0.9629		6.156	
	cc-pVQZ	2.953	2	3.378		0.99936		2.228		0.9508		9.907	
	cc-pV5Z	3.338	3	4.385		0.99936		2.227		0.9426		12.205	
	extrapol. σ_e [a]			4.458		0.99935		2.248		0.9410		12.491	
	extrapol. σ_0 [a]	3.413				0.99925		2.419		0.9416		8.235	
	aug-cc-pVDZ	12.699		8.523		*0.99949*	*1*	*1.994*	*1*	1.0040	2	−9.126	
	aug-cc-pVTZ	3.557		2.492	4	0.99942	2	2.125	2	0.9607		6.483	
	aug-cc-pVQZ	*2.914*	*1*	3.488		0.99938	4	2.192	4	0.9508		10.050	
	aug-cc-pV5Z	3.338	4	4.412		0.99937	5	2.210	5	0.9425		12.237	
	extrapol. σ_e [a]			4.559		0.99938		2.202		0.9418		12.47	
	extrapol. σ_0 [a]	3.365				0.99927		2.389		0.9424		8.216	

Table 9. Statistical parameters of linear regressions for HF calculated ^{13}C shieldings versus ZPV corrected experimental values σ_e^{exp} (7 data points all carbons exept **6**).

[a] Regressions with shieldings obtained from extrapolation of Dunning basis sets collected in Table 8.

mark value of 194.8 ppm of Table 7. The corresponding MP2 value of 201.16 or 200.50 ppm is in full agreement to the MP2 calculation of Gauss and Stanton [5] (see footnote on p. 1163), but off by 2 ppm from the experimental estimate of σ_e with 198.9 ppm. The B3LYP values are definitely much too small.

From the average values of deviations (av. $|\Delta\sigma|$) shown in Table 8, the general conclusion may be drawn that the Dunning HF limit values are closer to experimental σ_0 values than to estimated σ_e^{exp}, but MP2 limits are better approximations to the latter parameter. Average B3LYP limit values are too small by 11 to 16 ppm.

Linear regressions of ^{13}C shieldings

Statistical parameters and ratings of linear regressions for our calculations with ZPV corrected experimental σ_e^{exp} values are shown in Table 9 for the HF

	Basis set	av. $\Delta\sigma_0$ [ppm]	Rank	av. $\Delta\sigma_e$ [ppm]	Rank	R	Rank	esd [ppm]	Rank	m	Rank	b [ppm]	Rank
MP2	6-31G	28.329		24.153		0.99960		1.772		1.1473		−48.412	
	6-31G*	23.037		18.862		0.99975		1.400		1.1230		−38.477	
	6-31G**	22.794		18.618		0.99964		1.664		1.1390		−40.751	
	6-31++G**	22.708		18.532		0.99969		1.554		1.1305		−39.298	
	6-311G	16.946	5	12.771	5	0.99975		1.406		1.0411	5	−19.070	5
	6-311G*	12.636	4	8.461	4	0.99987	5	1.010	5	1.0270	2	−12.486	4
	6-311G**	10.997	3	6.821	3	*0.99993*	*1*	*0.755*	*1*	1.0353	4	−12.020	3
	6-311++G**	10.473	2	6.297	2	0.99991	3	0.840	3	1.0285	3	−10.482	2
	cc-pVDZ	23.216		19.040		0.99987	4	1.002	4	1.1056		−35.900	
	cc-pVTZ	*10.117*	*1*	*5.941*	*1*	0.99992	2	0.812	2	*1.0185*	*1*	−8.646	1
	aug-cc-pVDZ	21.414		17.238		0.99956		1.853		1.1058		−33.929	
	aug-cc-pVTZ [a]	9.864	–	5.554	–	0.99991	–	0.734	–	1.0083	–	−6.875	–
B3LYP	6-31G	9.741		5.565		0.99925		2.424		1.0612		−14.513	
	6-31G*	5.923		4.244	5	0.99893		2.888		1.0860		−13.843	
	6-31G**	7.070		3.602	4	0.99923		2.455		1.0724		−13.288	
	6-31++G**	7.170		3.424	3	0.99909		2.660		1.0660		−12.476	5
	6-311G	*1.936*	*1*	4.783		0.99915		2.565		0.9649		9.547	3
	6-311G*	5.061	2	9.237		*0.99949*	*1*	*1.996*	*1*	*0.9821*	*1*	11.586	4
	6-311G**	5.419	3	9.595		0.99938	4	2.197	4	0.9695	3	13.594	
	6-311++G**	6.067		10.242		0.99931		2.319		0.9625		15.134	
	cc-pVDZ	6.679		2.840	2	0.99931		2.323		1.0365		−7.720	2
	cc-pVTZ	5.710	4	9.886		0.99939	3	2.175	3	0.9695	2	13.875	
	cc-pVQZ	9.344		13.520		0.99932		2.294		0.9472		20.234	
	cc-pV5Z	11.197		15.373		0.99930		2.336		0.9347		23.549	
	extrapol. σ_e [b]			15.902		0.99928		2.375		0.9296		24.674	
	extrapol. σ_0 [b]	11.726				0.99960		1.768		0.9306		20.377	
	aug-cc-pVDZ	5.767	5	*2.364*	*1*	0.99881		3.049		1.0327	4	*−6.243*	*1*
	aug-cc-pVTZ	5.800		9.975		0.99947	2	2.024	2	0.9658	5	14.448	
	aug-cc-pVQZ	9.563		13.738		0.99936	5	2.240	5	0.9460		20.588	
	aug-cc-pV5Z [a]	10.693	–	15.003	–	0.99956	–	1.625	–	0.9160	–	26.670	–
	extrapol. σ_e [b]			16.016		0.99907		2.692		0.9347		24.153	
	extrapol. σ_0 [b]	11.841				0.99943		2.114		0.9357		19.8515	

Table 10. Statistical parameters of linear regressions for MP2 and B3LYP calculated ^{13}C shieldings, versus ZPV corrected experimental values σ_e^{exp} (7 data points except where noted).

[a] 6 data points; [b] regressions with shieldings obtained from extrapolation of Dunning basis sets collected in Table 8.

procedure and in Table 10 for MP2 and B3LYP methods. The mean absolute deviations are included for the experimental σ_0 shieldings (av. $|\Delta\sigma_0|$) and the ZPV corrected σ_e^{exp} shieldings (av. $|\Delta\sigma_e|$). With a few exceptions in the series of Dunning basis sets, the σ_e based deviations are smaller than σ_0 based values. Interestingly, Pople's triple-zeta 6-311G family yields significantly smaller deviations than the double-zeta 6-31G family. In Table 9, *R* and *esd*, the indicators of precision, show identical ranking. The five best rankings are found for Dunning basis sets with an optimum of 0.9995 for *R* and an *esd* of 1.994 ppm for HF/aug-cc-pVDZ calculations. Best values in Table 10 are $R = 0.9999$ with $esd = 0.755$ ppm for MP2/6-311G** shieldings and $R = 0.9995$ with $esd = 1.996$ ppm for B3LYP/6-311G* calculations. (Regressions with less than 7 data points have been omitted from the ranking.)

Best slopes (*m*) as indicators of accuracy are obtained by cc-pVDZ on the HF level shown in Table 9, and cc-pVTZ for MP2 and 6-311G* for B3LYP in Table 10. Intercepts (*b*) are relatively large at best 3.20, −8.65 and −6.24 ppm for HF, MP2 and B3LYP calculations. Actually, MP2 produces the most congruent results with all regression parameters showing similar trends.

Prediction of ^{13}C shieldings of butadiene

The extrapolation of Dunning basis set shieldings of Table 8 may be used with the HF regression equation in Table 9 to predict the unmeasured ^{13}C σ_0 shieldings of butadiene (**6**) as $C^1 = 70.83$ (69.52) ppm and $C^2 = 48.75$ (44.97) ppm. The values in parentheses are derived from the corresponding B3LYP regression of Table 10. They are closer to an experimental estimate from solution shifts *via* the equation on page 1158 and a TMS shielding of 188.1 ppm yielding $C^1 = 69.21$ ppm and $C^2 = 44.67$ ppm.

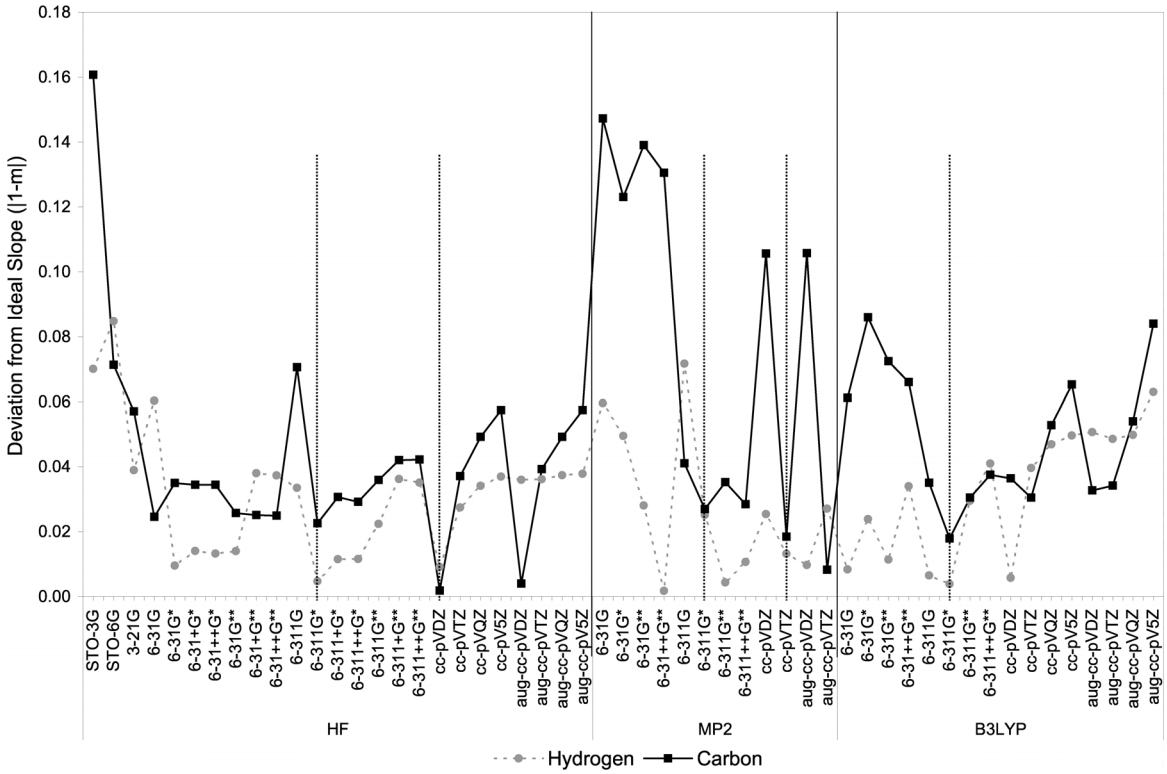

Fig. 6. Comparison of slopes *m* as indicator of accuracy of hydrogen and carbon shielding regressions for all methods and basis sets.

Combination of ^{1}H and ^{13}C findings

At first, the quite different statistics of hydrogen and carbon seem to make it difficult to recommend a single method suitable for the simultaneous optimal calculation of both ^{1}H and ^{13}C chemical shifts, respectively shieldings. However, the plain numbers are somewhat misleading.

Fig. 6 displays graphically the quality of the slopes of hydrogen and carbon shielding regressions. This quality is expressed by the closeness of the slope to the ideal value, naturally one. Picking coincidences of local minima of both nuclei[f] (marked in the figure by vertical dotted lines), one finds cc-pVDZ to be the first choice on the HF level, cc-pVTZ in the MP2 case, and 6-311G* for the B3LYP method. 6-311G* can also be taken as a compromise on the HF and MP2 levels of theory. The particular values are not always the best ones, but are at least of rank three, except for ^{1}H in the MP2 method.

[f]Equivalent, but less descriptive, is the harmonic average.

The estimated standard deviations depicted in Fig. 7 show a more complex behavior, to favor some basis sets is not as easy as for the slopes[g]. However, 6-311G* is of reasonable precision for HF and best for B3LYP. Other options with acceptable precision are HF/aug-cc-pVDZ, MP2/cc-pVTZ, and B3LYP/aug-cc-pV5Z, each one more expensive and of poorer accuracy defined by the slope.

Tetramethylsilane

With the simple equation $\delta = \sigma_{\mathrm{TMS}} - \sigma$, absolute shieldings can be converted into chemical shifts. As it is mandatory to calculate both shieldings with the same method and basis set, σ_{TMS} has to be calculated for all combinations of methods and basis sets to be considered.

Because no experimental r_{e} geometry of TMS is available, its geometry was optimized in each basis set. Only after finishing this work, an experi-

[g]Averaging is not possible here due to different domains of the errors.

Basis set	σ_C [ppm]	σ_C [ppm][a]	σ_H [ppm]	σ_H [ppm][a]	r_{SiC}[Å]	r_{CH} [Å]	α_{SiCH} [°]
STO-3G	249.4485		33.7573		1.8640	1.0821	111.4003
STO-6G	251.8526		34.1850		1.8578	1.0770	111.3952
3-21G	214.6567	213.5527	33.8334	33.5426	1.9183	1.0866	111.0370
6-31G	208.2360		33.6781		1.9173	1.0854	111.0441
6-31G*	201.7285	199.9853	32.9035	32.5976	1.8938	1.0874	111.4620
6-31+G*	201.8459	200.1609	32.8190	32.5272	1.8936	1.0879	111.4759
6-31++G*	202.1032		32.8185		1.8934	1.0880	111.4783
6-31G**	203.1555	201.3498	32.3358	32.0165	1.8926	1.0873	111.3708
6-31+G**	203.1713	201.3475	32.2849	31.9630	1.8927	1.0872	111.3807
6-31++G**	203.5056	201.6892	32.2918	31.9714	1.8925	1.0873	111.3775
6-311G	203.5439		33.6399		1.9038	1.0828	111.0421
6-311G*	195.9890	193.8951	32.8505	32.4911	1.8891	1.0863	111.5494
6-311+G*	195.9349		32.7994		1.8893	1.0865	111.5503
6-311++G*	196.1500		32.7887		1.8896	1.0865	111.5438
6-311G**	196.2165	194.3688	32.4875	32.1582	1.8882	1.0874	111.3161
6-311+G**	195.9187	194.1036	32.4645	32.1404	1.8882	1.0875	111.3125
6-311++G**	196.1819	194.3700	32.4549	32.1316	1.8884	1.0875	111.3098
B3LYP [a]		199.9853		32.5976	1.896	1.097	109.5
exp. [b]		188.1 [c]			1.877(4)	1.100(3)	111.0(2)

Table 11. Hartree-Fock calculated absolute shieldings of carbon and hydrogen of TMS and optimized geometries for the 17 Pople basis sets used in this work.

[a] Ref. [82], calculated with a geometry optimized using B3LYP/6-31G*; [b] ref. [47]; [c] ref. [46].

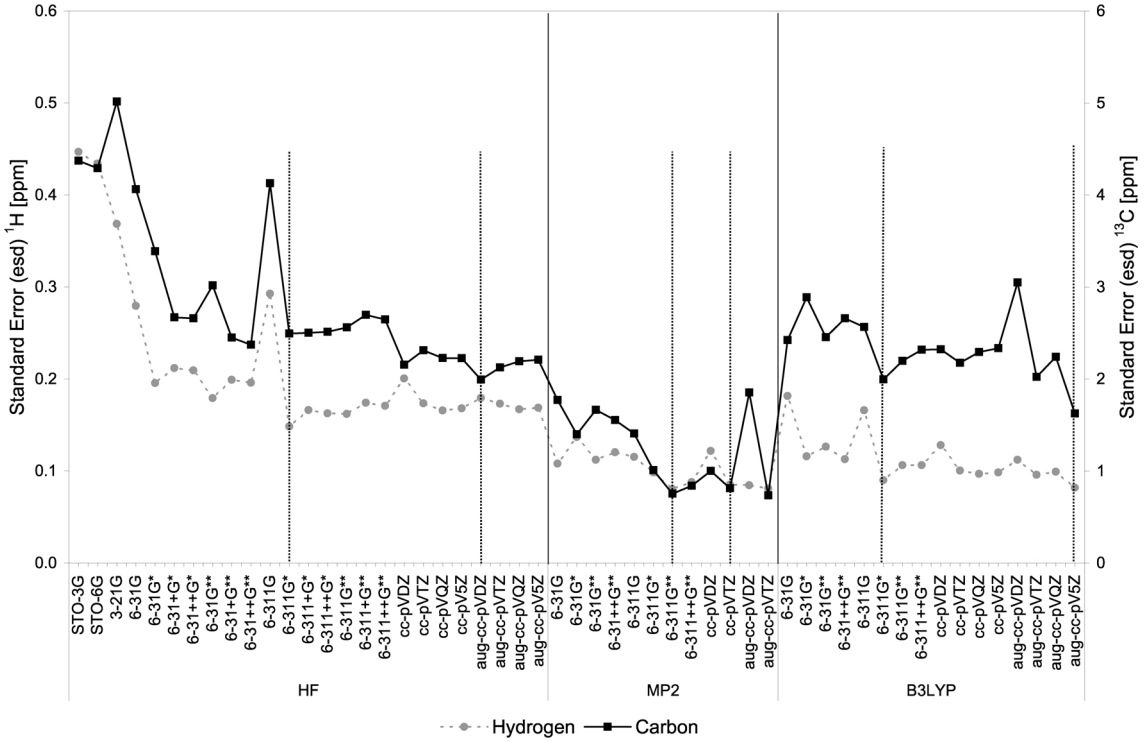

Fig. 7. Comparison of *esd* values as indicator of precision of hydrogen and carbon shielding regressions for all methods and basis sets.

mental ED r_g geometry of TMS was reported [47]. But as these optimizations introduce an unwanted geometry dependence to the resulting shifts, TMS shieldings and consequential relative chemical shift were calculated only on the HF level with 17 Pople basis sets. Our numerical results are presented in Table 11 in comparison to published TMS shieldings [82] for an arbitrarily fixed molecular geometry. These two TMS shieldings differ in a range of 0.32 ± 0.04 ppm.

Basis set	av. $\lvert\Delta\delta\rvert$ [ppm]	Rank	R	Rank	esd [ppm]	Rank	m	Rank	b [ppm]	Rank
STO-3G	0.732		0.98782		0.438		0.8929		−0.233	
STO-6G	0.948		0.98848		0.426		0.8788		−0.408	
3-21G	0.643		0.99192		0.357		0.9231		−0.327	
6-31G	0.694		0.99558		0.264		0.9028		−0.299	
6-31G*	0.359	1	0.99795		0.180		0.9701	1	−0.247	
6-31+G*	0.400	5	0.99796		0.180		0.9477		−0.202	
6-31++G*	0.396	4	0.99798		0.179		0.9484	5	−0.202	
6-31G**	0.361	2	0.99786		0.184		0.9470		−0.153	5
6-31+G**	0.431		0.99779		0.187		0.9242		−0.128	2
6-31++G**	0.434		0.99785		0.184		0.9249		−0.135	3
6-311G	0.730		0.99551		0.266		0.9290		−0.439	
6-311G*	0.431		0.99873	2	0.142	2	0.9652	2	−0.299	
6-311+G*	0.454		0.99865	3	0.146	3	0.9498	3	−0.262	
6-311++G*	0.435		0.99874	1	0.141	1	0.9498	4	−0.244	
6-311G**	0.396	3	0.99812		0.173		0.9388		−0.153	
6-311+G**	0.431		0.99812	5	0.172	5	0.9257		−0.136	4
6-311++G**	0.417		0.99820	4	0.169	4	0.9268		−0.126	1

Table 12. Statistical parameters of linear regressions for calculated ^{1}H chemical shifts versus experimental gas phase values of Table 2 (10 data points).

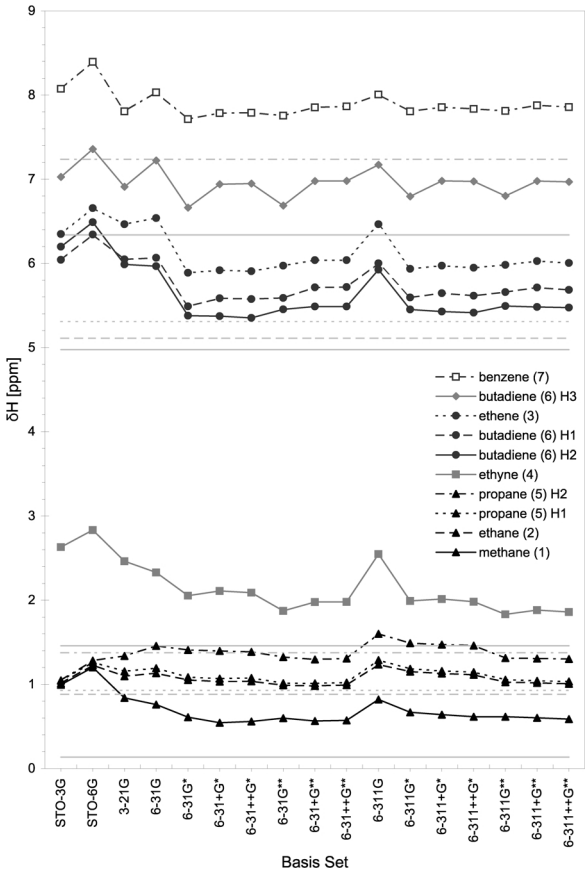

Fig. 8. HF calculated hydrogen chemical shifts (δ_H in ppm) of molecules **1 – 7** for 17 Pople basis sets, experimental values shown as gray lines.

Hydrogen chemical shifts

The strong basis set dependence of the before mentioned shieldings persists the conversion into relative shifts. The values shown in Fig. 8 spread in an interval of up to 1.1 ppm, a rather high divergence in relation to the total ^{1}H NMR scale of approximately 13 ppm, but the reduction of the interval compared to 2.1 ppm in the shielding case is a sign for a certain error cancellation.

Essential is the introduction of polarization functions on carbon. Neither the consecutive lowering of the shieldings shown in Fig. 4 on introduction of polarization functions on hydrogen in the 6-31G and 6-311G families is observed for shifts, nor the significant difference between these two families.

Considering the shape of the "graphs" in Fig. 8 (disregarding the position on the scale), the different hydrogen atoms of all molecules can roughly be divided into two groups: one representing the hydrogen atoms bonded to saturated carbon atoms (molecules **1**, **2**, and **5**) and another the ones bonded to unsaturated carbon (molecules **3**, **6**, and **7)**. Ethyne (**4**) and H^3 of butadiene (**6**) play a somewhat special role. This differentiation is also attributed to TMS, whose shieldings as a saturated molecule virtually coincide with those of methane.

In both groups, the minimal basis sets give unreliable bad shifts. In the first group, at least split-valence basis sets are required to differentiate between CH_4, CH_3, and CH_2 protons at tetrahedral carbon. In both groups, the deviations produced by the basis sets 6-31G and 6-311G are exceptional. It appears

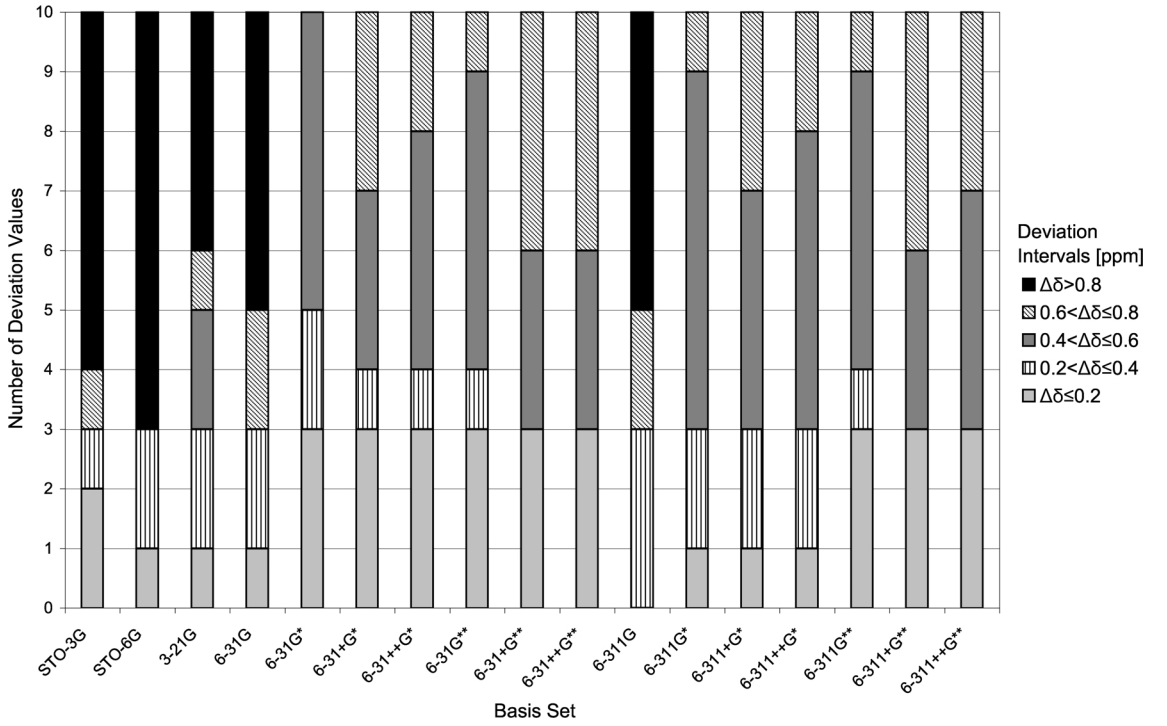

Fig. 9. Error statistics in equal steps of 0.2 ppm for deviations of calculated from experimental hydrogen chemical shifts (10 values).

necessary to add polarization functions at carbon to obtain reliable chemical shifts of hydrogen.

The absolute deviations of the calculated ^{1}H shifts from experimental gas phase values were classified into five equal intervals for each basis set. An error statistics for the number of values in these intervals is shown in Fig. 9. It can be seen that basis sets without polarization give many large errors, while there is a tendency towards smaller deviations on addition of polarization functions. Unexpectedly, triple-zeta basis sets (6-311G and its extensions) do not give more small deviations than double-zeta bases, only an increase of medium ones.

Table 12 shows the statistical parameters of linear regressions between calculated and experimental gas phase ^{1}H chemical shifts, along with the average absolute deviations. Comparing these shift and the shielding regressions of Table 5, again an error cancellation is obvious – the statistical parameters *R*, *esd*, and *m* are all slightly better for shifts than for shieldings. Regressions using TMS shieldings of constant geometry of Table 11 lead to the same statistics except for av. $|\Delta\delta|$ and intercepts *b*, which are both smaller.

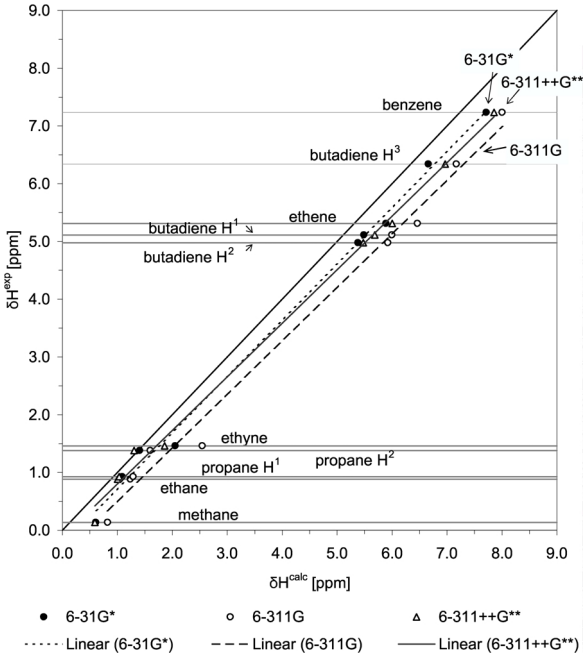

Fig. 10. Plot of some ^{1}H shift data (δ_H in ppm) and corresponding regression lines.

Basis set	av. $\lvert\Delta\delta\rvert$ [ppm]	Rank	R	Rank	esd [ppm]	Rank	m	Rank	b [ppm]	Rank
STO-3G	8.124		0.99714		4.716		1.1611		−15.833	
STO-6G	12.245		0.99724		4.634		1.0717		−16.830	
3-21G	4.108		0.99644		5.265		1.0575		−2.623	
6-31G	3.840		0.99756		4.360		0.9758	2	*−1.296*	*1*
6-31G*	2.778		0.99817		3.773		1.0354		−2.175	4
6-31+G*	2.295	3	0.99881		3.041		1.0349		−2.038	2
6-31++G*	2.309	4	0.99883		3.013		1.0349		−2.378	
6-31G**	2.379	5	0.99853		3.381		1.0262	5	−2.229	
6-31+G**	*1.993*	*1*	0.99899		2.800		1.0256	4	−2.078	3
6-31++G**	2.011	2	0.99906	2	2.702	2	1.0255	3	−2.412	
6-311G	6.781		0.99774		4.197		0.9300		−2.689	
6-311G*	3.777		0.99903	4	2.751	4	*0.9780*	*1*	−2.520	
6-311+G*	4.041		*0.99907*	*1*	*2.697*	*1*	0.9699		−2.364	
6-311++G*	4.308		0.99905	3	2.715	3	0.9713		−2.704	
6-311G**	4.332		0.99903	5	2.753	5	0.9646		−2.349	
6-311+G**	4.541		0.99896		2.843		0.9586		−2.210	5
6-311++G**	4.738		0.99900		2.786		0.9584		−2.389	

Table 13. Statistical parameters of linear regressions for calculated ^{13}C chemical shifts versus experimental gas phase values (7 data points).

The precision parameters both show 6-311G* and 6-311++G* as the most precise basis sets with largest *R* and smallest *esd*. Regarding the accuracy parameters, it is noticeable that basis sets with polarization functions on carbon give good slopes. Basis sets with additional polarization functions on hydrogen give significantly smaller intercepts, but slopes of poorer quality. This leads to 6-31G* as the most accurate basis set with a slope *m* of 0.970, which is in agreement to the smallest average shift deviations (av. $\lvert\Delta\delta\rvert$) of 0.368 ppm.

The experimental ^{1}H shifts are plotted against a subset of the calculated data in Fig. 10. Regression lines for three basis sets are shown as examples. Chosen are the one for 6-31G* for the best slope with moderate expense, 6-311G to show that polarization is more valuable than more splitting, and 6-311++G** for the most expensive calculation, but results of not correspondingly higher quality.

Carbon chemical shifts

Fig. 11 presents graphically the basis set dependence of ^{13}C chemical shifts in relation to experimental shifts, which may be compared to ^{13}C shieldings of Fig. 5. Shifts of saturated carbon atoms in **1**, **2** and **5** show only minor variations with increase of basis sets and no jump on introduction of polarization functions as from 6-31G to 6-31G* and from 6-311G to 6-311G*. All other carbon shifts reflect the importance of polarization functions on carbon while 6-31G and 6-311G shifts are clearly off from other values. Polarization at hydrogen and diffuse functions show only a small effect. An important difference between the 6-31G and 6-311G families is only present for unsaturated carbons. Individual calculated shifts vary with basis sets

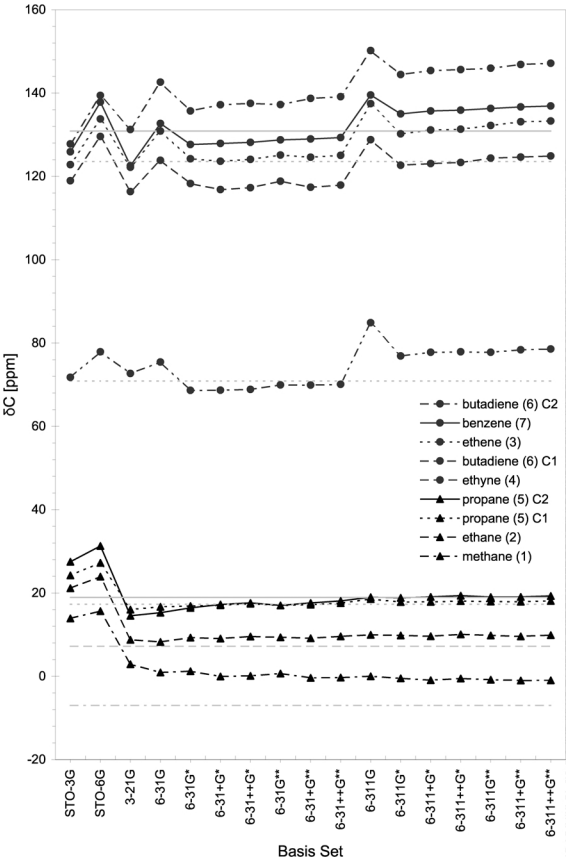

Fig. 11. HF calculated carbon chemical shifts (δ_C in ppm) of molecules **1 – 7** for 17 Pople basis sets, experimental values shown as gray lines.

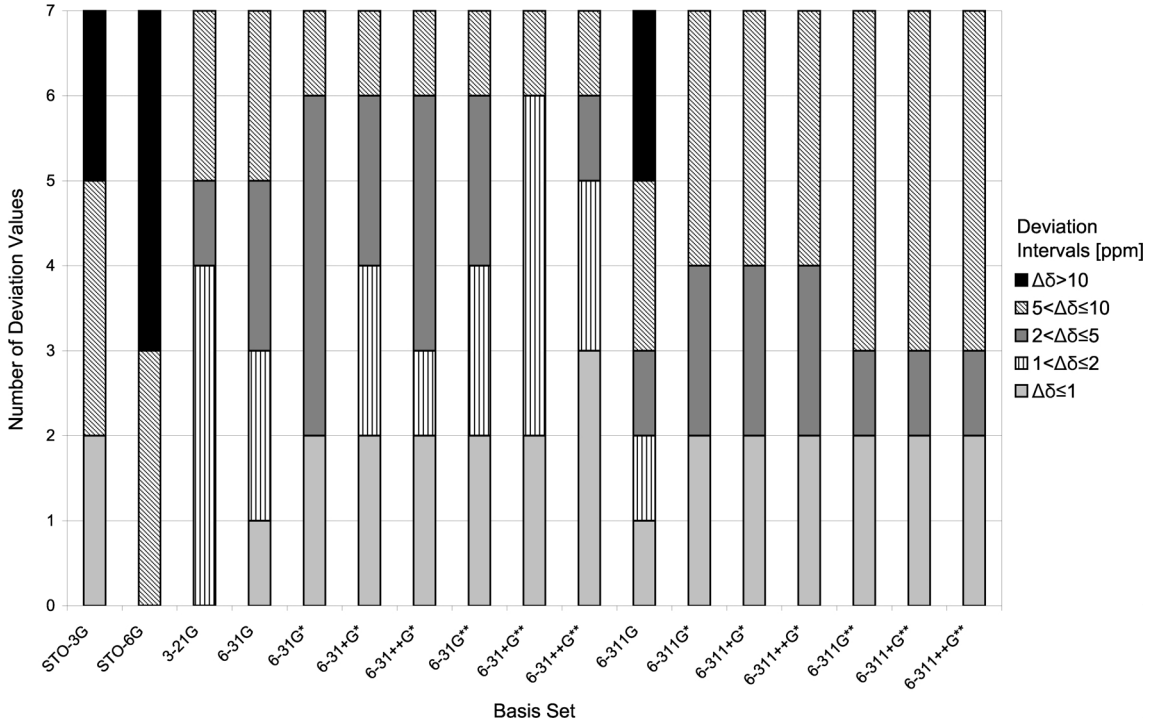

Fig. 12. Error statistics in increasing steps for deviations of calculated from experimental carbon chemical shifts (7 values).

in a range of 11 to 22 ppm for a total ^{13}C NMR scale of about 300 ppm.

The error statistics for deviations from experimental shifts distributed into five appropriate intervals is shown in Fig. 12.

The overall picture appears similar to hydrogen shifts; small basis sets result in many large deviations and larger basis sets tend to more small errors. Deviations for triple-zeta basis sets are noticeably larger than those for double-zeta basis sets, yet they appear more uniform.

The statistical values for regressions of ^{13}C gas phase data are collected in Table 13.

Similar to ^{1}H, the HF derived ^{13}C shift regressions yield better *R* and *esd* than for shieldings, but they give slightly worse slopes.

Here, according to *R* and *esd*, the best (most precise) basis set is 6-311+G*. Consequently this is the most promising candidate for highly accurate shift predictions through empirical scaling. The slope indicates 6-311G* as the best (most accurate) basis set, yet a lower average deviation is obtained with the smaller basis set 6-31+G**. Noticeably, the whole extended triple-zeta series improves the slopes with respect to the double-zeta 6-31G series, but produces greater average deviations.

Conclusions

The accurate and precise *ab initio* calculation of NMR parameters is of great interest to experimentalists. To give a potential user assistance in the difficult task of choosing a suitable method, we examined three theoretical methods (HF, MP2, and B3LYP) and 17 of Pople's basis sets and 8 of Dunning's type and determined their quality by statistical linear regressions. The newly developed, easy to use flow NMR technique for measuring experimental gas phase ^{1}H NMR spectra delivered reliable reference values.

For evaluation of absolute shieldings it is essential to differentiate between experimental σ_0 values which refer to vibrating and rotating molecules at about 300 K, and our calculated σ_e shieldings referring to the frozen r_e geometry at 0 K. To treat this rovibrational effect, we applied ZPV corrections from ref. [42] to derive σ_e^{exp} values for statistical comparison to the calculated shieldings. The correlation with these yielded better statistical parameters.

Table 14. Collection of best basis sets with derived regression parameters (*R*, *esd*, *m*, and *b*) for each calculational method (HF, MP2, B3LYP) and for each kind of considered experimental parameter (gas phase shieldings σ_0, ZPV corrected shieldings σ_e^{exp}, and chemical shifts δ for ^{1}H and ^{13}C).

Atom type	Correlation[a]	Statistical indicator	HF		MP2		B3LYP	
^{1}H	σ^{calc}/σ_0	av. $\lvert\Delta\sigma_0\rvert$	aug-cc-pV5Z	0.972	cc-pVTZ	0.821	cc-pV5Z	0.748
		R	6-311++G*	0.99874	aug-cc-pVDZ	0.99959	6-311G*	0.99948
	Tables	esd	6-311++G*	0.141	aug-cc-pVDZ	0.081	6-311G*	0.091
	S3 and S4	m	6-31G*	0.9701	6-31G*	1.0084	6-31G*	0.9834
		b	6-311G	-0.064	6-31++G**	0.158	cc-pVDZ	0.383
	$\sigma^{calc}/\sigma_e^{exp}$	av. $\lvert\Delta\sigma_e\rvert$	aug-cc-pV5Z	0.398	cc-pVTZ	0.247	cc-pV5Z	0.211
		R	6-311G*	0.99871	6-311G**	0.99962	6-311G*	0.99953
	Tables	esd	6-311G*	0.148	6-311G**	0.080	6-311G*	0.090
	5 and 6	m	6-311G*	1.0047	6-31++G**	0.9982	6-311G*	1.0039
		b	6-31G	0.125	aug-cc-pVDZ	−0.106	6-31G**	−0.153
	$\delta^{calc}/\delta^{exp}$	av. $\lvert\Delta\delta\rvert$	6-31G*	0.359				
		R	6-311++G*	0.99874				
	Table 12	esd	6-311++G*	0.141				
		m	6-31G*	0.9701				
		b	6-311++G**	−0.126				
^{13}C	σ^{calc}/σ_0	av. $\lvert\Delta\sigma_0\rvert$	aug-cc-pVQZ	2.914	cc-pVTZ	10.117	6-311G	1.936
		R	aug-cc-pVDZ	0.99936	6-311++G**	0.99995	6-311G*	0.99976
	Tables	esd	aug-cc-pVDZ	2.233	6-311++G**	0.605	6-311G*	1.361
	S7 and S8	m	cc-pVDZ	0.9987	cc-pVTZ	1.0192	6-311G*	0.9831
		b	6-311++G*	0.275	cc-pVTZ	−12.933	6-311G	5.231
	$\sigma^{calc}/\sigma_e^{exp}$	av. $\lvert\Delta\sigma_e\rvert$	6-311G*	2.219	cc-pVTZ	5.941	aug-cc-pVDZ	2.364
		R	aug-cc-pVDZ	0.99949	6-311G**	0.99993	6-311G*	0.99949
	Tables	esd	aug-cc-pVDZ	1.994	6-311G**	0.755	6-311G*	1.996
	9 and 10	m	cc-pVDZ	0.9982	cc-pVTZ	1.0185	6-311G*	0.9821
		b	6-311G*	3.204	cc-pVTZ	−8.646	aug-cc-pVDZ	−6.243
	$\delta^{calc}/\delta^{exp}$	av. $\lvert\Delta\delta\rvert$	6-31+G**	1.993				
		R	6-311+G*	0.99907				
	Table 13	esd	6-311+G*	2.697				
		m	6-311G*	0.9780				
		b	6-31G	−1.296				

[a] Tables S3, S4, S7, and S8 are contained in supplementary material at http://www.uni-tuebingen.de/uni/coh → Publications.

We found that basis sets without polarization functions are inappropriate choices for exact calculations, yet there is no simple relation between the number of basis functions and the quality of the shifts. In Table 14, we present the basis sets leading to best statistical parameters for each kind of correlation. The quantitatively best basis set is not uniquely defined. It depends on selected methods, experimental references and considered regression parameters.

For calculations of molecular magnetic properties, Schleyer *et al.* [83] suggested to "choose the highest reasonable possible level of theory". They selected the 6-311++G** basis set for this. Our statistical evaluation shows that best *R* and *esd* parameters as indicators of precision, which are always strictly correlated, are found for this basis set only in the case of ^{13}C σ_0 based shieldings within the MP2 method. This is reasonable because this post-HF calculation needs a high degree of flexibility.

The less elaborate 6-311++G* basis set yields best *esd* values for ^{1}H σ_0 based shieldings and chemical shifts δ_H in the HF approach. 6-311+G* is the best choice for HF calculated ^{13}C chemical shifts and 6-311G** shows lowest *esd* for σ_e^{exp} based ^{13}C shieldings in the MP2 approach. However, 6-311G* is the basis set which is found with best *esd* in most cases: All shieldings calculated with the hybrid DFT functional B3LYP and the σ_e based ^{1}H shieldings in the HF method. Numerical best *esd* values determine the sequence of increasing precision from HF (0.14 ppm) over B3LYP (0.09 ppm) to MP2 (0.08 ppm) for ^{1}H shieldings and the same order for ^{13}C.

Surprisingly, best slopes *m* as indicators of accuracy of the model are already found for the relatively small 6-31G* basis set within all applied methods for the regressions with ^{1}H σ_0 shieldings and HF chemical shifts. This is an agreement with Schleyer's recommendation of 1996 introducing the nucleus indepen-

dent chemical shift (NICS) calculations as a probe of aromaticity [84].

Average deviations between calculated and experimental values (av. $|\Delta x|$) of Table 14 are with two exceptions lowest for different basis sets of the Dunning series, especially cc-pVTZ.

For HF and B3LYP, three consecutive calculations with Dunning basis sets could be exponentially extrapolated to determine basis set limits of ^{1}H and ^{13}C shieldings. For ^{1}H shieldings, average deviations are smallest for these limits.

The selection of best basis sets presented in Table 14 may be misleading as the numerical differences between the five foremost basis sets indicated by rankings in the appropriate tables of this paper and the supplementary material are not too big. For example, the 6-311G* basis set occurs relatively often ranking second with hardly poorer quality.

For any basis set of our selection, the corresponding regression equation can be used to correct a calculated σ_e shielding of ^{1}H or ^{13}C to a predicted shielding or chemical shift which can be compared to experiment.

As a general conclusion, the 6-311G* basis set may be recommended for simultaneous GIAO calculations of ^{1}H and ^{13}C with both high precision and accuracy in the HF and B3LYP methods. For MP2 calculations, a larger basis set between 6-311G** and 6-311++G** or cc-pVTZ is advisable, but diffuse functions are not essential.

Acknowledgements

The authors wish to thank Dr. Heidrun Händel for assistance with WIN-DAISY.

[1] L. M. Jackman, S. Sternhell, "Applications of Nuclear Magnetic Resonance Spectroscopy in Organic Chemistry", 2nd ed., Pergamon Press, Oxford (1969).
[2] H. Günther, "NMR-Spektroskopie", 3rd ed., Thieme, Stuttgart (1992).
[3] J. K. M. Sanders, B. K. Hunter, "Modern NMR Spectroscopy. A Guide for Chemists", Oxford University Press (1987).
[4] T. Helgaker, M. Jaszunski, K. Ruud, "Ab Initio Methods for the Calculation of NMR Shielding and Indirect Spin-Spin Coupling Constants", Chem. Rev. **99**, 293 (1999).
[5] J. Gauss, J. F. Stanton, "Electron-Correlated Approaches for the Calculation of NMR Chemical Shifts", Adv. Chem. Phys. **123**, 355 (2002).
[6] M. Kaupp, M. Bühl, V. G. Malkin (Eds.), "Calculation of NMR and EPR Parameters, Theory and Applications", Wiley-VCH, Weinheim (2004).
[7] N. F. Ramsay, Phys. Rev. **78**, 699 (1950).
[8] W. Kutzelnigg, Isr. J. Chem. **19**, 193 (1980).
[9] M. Schindler, W. Kutzelnigg, J. Chem. Phys. **76**, 1919 (1982).
[10] A. E. Hansen, T. D. Bouman, J. Chem. Phys. **82**, 5035 (1985).
[11] T. A. Keith, R. F. W. Bader, Chem. Phys. Lett. **210**, 223 (1993).
[12] F. London, Naturwissenschaften **15**, 187 (1937).
[13] F. London, J. Phys. Radium **8**, 397 (1937).
[14] R. Ditchfield, Chem. Phys. Lett. **15**, 203 (1972).
[15] R. Ditchfield, Mol. Phys. **27**, 789 (1974).
[16] K. Wolinski, J. F. Hinton, P. Pulay, J. Am. Chem. Soc. **112**, 8251 (1990).
[17] Gaussian 98, Revision A.7, M. J. Frisch, G. W. Trucks, H. B. Schlegel, G. E. Scuseria, M. A. Robb, J. R. Cheeseman, V. G. Zakrzewski, J. A. Montgomery (Jr.), R. E. Stratmann, J. C. Burant, S. Dapprich, J. M. Millam, A. D. Daniels, K. N. Kudin, M. C. Strain, O. Farkas, J. Tomasi, V. Barone, M. Cossi, R. Cammi, B. Mennucci, C. Pomelli, C. Adamo, S. Clifford, J. Ochterski, G. A. Petersson, P. Y. Ayala, Q. Cui, K. Morokuma, D. K. Malick, A. D. Rabuck, K. Raghavachari, J. B. Foresman, J. Cioslowski, J. V. Ortiz, A. G. Baboul, B. B. Stefanov, G. Liu, A. Liashenko, P. Piskorz, I. Komaromi, R. Gomperts, R. L. Martin, D. J. Fox, T. Keith, M. A. Al-Laham, C. Y. Peng, A. Nanayakkara, C. Gonzalez, M. Challacombe, P. M. W. Gill, B. Johnson, W. Chen, M. W. Wong, J. L. Andres, C. Gonzalez, M. Head-Gordon, E. S. Replogle, J. A. Pople, Gaussian, Inc., Pittsburgh PA (1998).
[18] D. B. Chesnut, C. K. Foley, J. Chem. Phys. **84**, 852 (1986).
[19] D. B. Chesnut, C. G. Phung, J. Chem. Phys. **91**, 6238 (1989).
[20] D. B. Chesnut, D. W. Wright, J. Comput. Chem. **12**, 546 (1991).
[21] C. M. Rohlfing, L. C. Allen, R. Ditchfield, Chem. Phys. **87**, 9 (1984).
[22] H. Fukui, T. Baba, H. Matsuda, K. Miura, J. Chem. Phys. **100**, 6608 (1994).
[23] J. R. Cheeseman, G. W. Trucks, T. A. Keith, M. J. Frisch, J. Chem. Phys. **104**, 5497 (1996).
[24] D. B. Chesnut, Chem. Phys. **214**, 73 (1997).
[25] W. J. Hehre, L. Radom, P. v. R. Schleyer, J. A. Pople, "Ab initio Molecular Orbital Theory", Wiley-Interscience, New York (1986).
[26] W. Koch, M. C. Holthausen, "A Chemists Guide to Density Functional Theory", Wiley/VCH, New York/Weinheim (1999).
[27] D. A. Forsyth, A. B. Sebag, J. Am. Chem. Soc. **119**, 9483 (1997).

[28] I. Alkorta, J. Elguero, New J. Chem. 381 (1998).
[29] K. B. Wiberg, J. Comput. Chem. **20**, 1299 (1999).
[30] P. R. Rablen, S. A. Pearlman, J. Finkbiner, J. Phys. Chem. A **103**, 7357 (1999).
[31] K. B. Wiberg, J. D. Hammer, K. W. Zilm, J. R. Cheeseman, J. Org. Chem. **64**, 6394 (1999).
[32] C. Møller, M. S. Plesset, Phys. Rev. **46**, 618 (1934).
[33] J. Gauss, J. Chem. Phys. **99**, 3629 (1993).
[34] J. Gauss, Chem. Phys. Lett. **229**, 198 (1994).
[35] J. Gauss, J. F. Stanton, J. Chem. Phys. **102**, 251 (1995).
[36] J. Gauss, J. F. Stanton, J. Chem. Phys. **103**, 3561 (1995).
[37] J. Gauss, J. F. Stanton, J. Chem. Phys. **104**, 2574 (1996).
[38] K. Ruud, T. Helgaker, R. Kobayashi, P. Jørgensen, K. L. Bak, H. J. Aa. Jensen, J. Chem. Phys. **100**, 8178 (1994).
[39] W. T. Raynes, P. W. Fowler, P. Lazzeretti, R. Zanasi, M. Grayson, Mol. Phys. **64**, 143 (1988).
[40] D. Sundholm, J. Gauss, A. Schäfer, J. Chem. Phys. **105**, 11051 (1996).
[41] K. Ruud, P.-O. Åstrand, P. R. Taylor, J. Chem. Phys. **112**, 2668 (2000).
[42] K. Ruud, P.-O. Åstrand, P. R. Taylor, J. Am. Chem. Soc. **123**, 4826 (2001).
[43] J. Vaara, K. Ruud, O. Vahtras, J. Chem. Phys. **41**, 2900 (1999).
[44] R. Cammi, B. Mennucci, J. Tomasi, J. Chem. Phys. **110**, 7627 (1999).
[45] K. Jackowski, W. T. Raynes, Mol. Phys. **34**, 465 (1977).
[46] A. K. Jameson, C. J. Jameson, Chem. Phys. Lett. **134**, 461 (1987).
[47] A. R. Campanelli, F. Ramondo, A. Domenicano, I. Hargittai, Struct. Chem. **11**, 155 (2000).
[48] J. Gauss, Ber. Bunsenges. Phys. Chem. **99**, 1001 (1995).
[49] L. Olsson, D. Cremer, J. Chem. Phys. **105**, 8995 (1996).
[50] B. Wang, U. Fleischer, J. F. Hinton, P. Pulay, J. Comput. Chem. **22**, 1887 (2001).
[51] J. Gauss, J. Chem. Phys. **116**, 4773 (2002).
[52] H. C. Dorn, in D. M. Grant, R. K. Harris (eds): Encyclopedia of Nuclear Magnetic Resonance, p. 2026 – 2037, Wiley, Chichester (1996).
[53] G. Häfelinger, C. U. Regelmann, T. M. Krygowski, K. Wozniak, J. Comput. Chem. **10**, 329 (1989).
[54] G. Häfelinger, in R. Zalewski, T. M. Krygowski, J. Shorter (eds): Similarity Models in Organic Chemistry, Biochemistry and Related Fields, p. 177 – 229, Elsevier, Amsterdam (1991).
[55] A. Neugebauer, G. Häfelinger, J. Mol. Struct. (Theochem) **578**, 229 (2002).
[56] A. Neugebauer, G. Häfelinger, J. Mol. Struct. (Theochem) **585**, 35 (2002).
[57] L. S. Bartell, H. K. Kuchitsu, J. Chem. Phys. **68**, 1213 (1978).
[58] J. L. Duncan, D. C. McKean, A. J. Bruce, J. Mol. Spectrosc. **74**, 361 (1979).
[59] J. L. Duncan, Mol. Phys. **28**, 1177 (1974).
[60] W. J. Lafferty, R. J. Thibault, J. Mol. Spectrosc. **14**, 79 (1964).
[61] J. Gauss, J. F. Stanton, J. Phys. Chem. A **104**, 2865 (2000).
[62] M.-N. Homsi, Dissertation, Universität Tübingen (1999).
[63] M. J. Frisch, J. A. Pople, J. S. Binkley, J. Chem. Phys. **80**, 3265 (1984).
[64] T. H. Dunning, Jr., J. Chem. Phys. **90**, 1007 (1989).
[65] A. D. Becke, J. Chem. Phys. **98**, 5648 (1993).
[66] P. J. Stephens, F. J. Devlin, C. F. Chabalowski, M. J. Frisch, J. Phys. Chem. **98**, 11623 (1994).
[67] W. T. Raynes, Nucl. Magn. Reson. **7**, 25 (1977).
[68] L. V. Vilkov, V. S. Mastrynkov, N. I. Sadova, "Determination of the Geometrical Structure of Free Molecules", Mir Publ., Moscow (1983).
[69] Y. Morino, K. Kuchitsu, T. Oka, J. Chem. Phys. **37**, 1108 (1963).
[70] M. Fink, C. W. Schmiedekamp, D. Gregory, J. Chem. Phys. **71**, 5238 (1976).
[71] C. J. Jameson, A. C. de Dios, Nucl. Magn. Reson. **31**, 64 (2001).
[72] D. E. Woon, T. H. Dunning, Jr., J. Chem. Phys. **99**, 1914 (1993).
[73] D. Feller, J. Chem. Phys. **96**, 6104 (1992).
[74] W. Kloppert, K. L. Bak, P. Jørgensen, J. Olsen, T. Helgaker, J. Phys. B: At. Mol. Opt. Phys. **32**, R103 (1999).
[75] A. Neugebauer, Dissertation, Universität Tübingen (2002).
[76] A. Neugebauer, G. Häfelinger, J. Phys. Org. Chem. submitted (2004).
[77] C. J. Guare, J. Chem. Educ. **68**, 649 (1991).
[78] W. T. Raynes, R. McVay, S. J. Wright, J. Chem. Soc. Faraday Trans. 2 **85**, 759 (1989).
[79] P. Lazzeretti, R. Zanasi, A. J. Sadlej, W. T. Raynes, Mol. Phys. **62**, 605 (1987).
[80] A. M. Lee, N. C. Handy, S. M. Colwell, J. Chem. Phys. **103**, 10095 (1995).
[81] P. J. Wilson, R. D. Amos, N. C. Handy, Chem. Phys. Letters **312**, 475 (1999).
[82] J. B. Foresman, Æ. Frisch, "Exploring Chemistry with Electronic Structure Methods", 2nd ed., Gaussian, Inc., Pittsburgh PA (1996).
[83] M. K. Cyranski, T. M. Krygowski, A. R. Katritzky, P. v. R. Schleyer, J. Org. Chem. **67**, 1333 (2002).
[84] P. v. R. Schleyer, C. Maerker, A. Dransfeld, H. Jiao,

N. J. R. van Eikema Hommes, J. Am. Chem. Soc. **118**, 6317 (1996).
[85] C. Suarez, N. S. True, B. E. Weiss, Bol. Soc. Chil. Quim. **34**, 15 (1989).
[86] H. Spiesecke, W. G. Schneider, J. Chem. Phys. **35**, 722 (1961).
[87] L. Petrarkis, C. H. Sederholm, J. Chem. Phys. **35**, 1175 (1961).
[88] K. Jackowski, M. Wilczek, M. Pecul, J. Sadlej, J. Phys. Chem. **104**, 5955 and 9806 (2000).
[89] P. Lazzeretti, M. Malagoli, R. Zanasi, J. Mol. Struct. (Theochem) **234**, 127 (1991).
[90] B. Bennett, W. T. Raynes, Magn. Reson. Chem. **29**, 946 (1991).
[91] U. Fleischer, W. Kutzelnigg, P. Lazzeretti, V. Mühlenkamp, J. Am. Chem. Soc. **116**, 5298 (1994).